DIBENZOYLMETHANE INDUCED CELL CYCLE ARREST IN HUMAN COLON CANCER CELLS AND ITS PHARMACOKINETIC DISPOSITION IN THE RATS

by

JIN-LIERN HONG

A Thesis submitted to the

Graduate School-New Brunswick

Rutgers, The State University of New Jersey

in partial fulfillment of the requirements

for the degree of

Master of Science

Graduate Program in Pharmaceutical Science

written under the direction of

Professor Ah-Ng Tony Kong, Ph.D.

and approved by

_____

_____

_____

_____

New Brunswick, New Jersey

May, 2007

ABSTRACT OF THE THESIS

DIBENZOYLMETHANE INDUCED CELL CYCLE ARREST IN HUMAN COLON CANCER CELLS AND ITS PHARMACOKINETIC DISPOSITION IN THE RATS

by JIN-LIERN HONG

Thesis Director: Professor Ah-Ng Tony Kong

The phytochemical dibenzoylmethane (DBM) is a minor constituent of licorice and has been shown to inhibit the growth of various types of cancer cells *in vitro* and prevent the carcinogenesis in various animal models. In previous studies in our laboratory it was found that DBM effectively inhibited colorectal carcinogenesis in APC(Min/+) mice. However, little is known regarding the cellular and molecular mechanisms underlying this inhibition, and the pharmacokinetic disposition of DBM still remains unclear. In the first part of this thesis, the anti-proliferative activity of DBM in human colon carcinoma HT-29 cells and the possible molecular mechanisms were investigated. We found that DBM inhibited HT-29 cell proliferation and that this inhibition is associated with cell cycle arrest at G_1 phase without inducing apoptosis. DBM-treatment dose-dependently down-regulated various cell cycle regulatory proteins including Cyclin D1, c-Myc and the phosphorylation of retinoblastoma protein. It appears that decreased mRNA transcription and proteasome-mediated protein degradation were involved in the DBM-induced down-regulation of those proteins. At

the same time, $p21^{CIP1}$, a negative cell cycle regulatory protein, was up-regulated by DBM at both protein and mRNA levels. Taken together, our results from this cell culture studies suggest that DBM inhibited HT-29 cell growth by modulating cell cycle regulatory proteins leading to the induction of cell cycle arrest. In the second part of my thesis, I developed and validated a rapid and sensitive high-performance liquid chromatography (HPLC) assay to determine the concentrations of DBM in the rat plasma, then followed by examining the *in vivo* pharmacokinetics of DBM in the rats by using this HPLC assay with UV detector. The data indicate that DBM followed a linear pharmacokinetics within the dose ranges tested. The volume of distribution at steady state was about 7.1 L with a systemic clearance of 0.72 L/Kg and $t_{1/2}$ of 13.23 hr. The oral bioavailability of DBM was approximately 11%. In summary, this thesis investigated the *in vitro* molecular mechanism of DBM-induced cell cycle arrest in HT-29 cells as well as the in vivo pharmacokinetic disposition of DBM in the rats.

ACKNOWLEDGEMENT

First of all, I would like to express my grateful thanks to my advisor, Dr. Ah-Ng Tony Kong, for his encourage and support throughout this work. I also acknowledge Drs. Bandaru Reddy and Mou-Tuan Huang who serve as my thesis committee for their valuable comments.

I owe my most sincere gratitude to Drs. Siwang Yu and Guoxiang Shen who kept an eye on the progress of my work and always was available when I needed their advises. During this work I have collaborated with many colleagues and I wish to extend my warmest thanks to all those for their kindness and invaluable help, in particular Tin Oo Khor, Wen Lin, Sujit Nair, Young-Sam Keum, Auemduan Prawan, Xiaoling Yuan, Wenge Li, Jung-Hwan Kim, Mohit Raja Jain and Ki-Han Kwon. My special thanks go to Ms. Hui Pung for her administrative assistance during past three years.

Finally, I would like to thank my parent, brother and sister. Without their encouragement and support, it would have been impossible for me to finish this work.

DEDICATION

To My Parents

TABLE OF CONTENTS

LIST OF TABLES

LIST OF FIGURES

CHAPTER 1

Literature Review

1.1 Concept of Cancer Chemoprevention

Cancer chemoprevention is a cancer preventive strategy which uses naturally occurring or synthetic chemical agents to prevent or reverse the process of carcinogenesis, or enhance the regression of abnormal cells or tissues to possibly normality with minimal or no side-effect [1]. It has been demonstrated that carcinogenesis process involves multiple stages: beginning with initiation, followed by an intermediate stage of promotion, from which evolves the stage of progression [2]. Epidemiological studies indicate that diet plays an important role in the risk of cancer. People who consume relatively larger amount of vegetables, fruits, and other plant products have a significantly lower cancer incidence [3]. A lot of natural compounds from our diet or sources of the diet have been found to effectively prevent cancer by interfering with the carcinogenesis processes [1]. For examples, sulforaphane from broccoli, resveratrol from grape, genistein from soy, curcumin from tumeric powder, epigallocatechin-3-gallate (EGCG) from green tea and isothiocyanates from cruciferous vegetables have been shown to possess cancer protective properties.

Chemopreventive agents can be categorized into blocking agents or suppressing

agents based on the carcinogenesis stage they target. Blocking agents, which act on the initiation stage, prevent the formation of reactive carcinogens, and/or prevent them from reaching the target sites or interacting with crucial cellular macro molecules such as DNA, RNA and proteins. On the other hand, suppressing agents inhibit or retard the promotion and progression of precancerous cell into malignant ones. Further studies elucidated that these various molecular processes can be regulated by these chemopreventive agents to inhibit carcinogenesis. For example, phenethyl isothicyanate (PEITC) and indole-3-carbinol (I3C) have been shown to act as ligands of the nuclear receptors to modify the induction of CYP enzymes [4]; and Epigallocatechin gallate (EGCG), Curcumin and Sulforaphane have been reported to suppress the activation of NF-kB and AP1 [1]. Currently, more than 40 chemopreventive agents are under clinical evaluation and more compounds are expected to emerge in the future [5].

1.2 Introduction of Colon Cancer

1.2.1 Statistics and epidemiology of colon cancer

Colorectal cancer is one of the major public health problems in the United States and other developed countries. Colorectal cancer occurs with similar frequency in men and women, and has higher incidence rates in the developed countries like North America,

Western Europe, and Australia/New Zealand, than in developing countries like Africa and Asia [6]. It was estimated that there were 1 million new cases around the world in 2002 (9.4% of the world total) and about 529,000 people died from this disease. In the United States, colorectal cancer is the third most common cancer in both men and women. This cancer is estimated to occur in 148,610 people (10% of USA total) and cause 55170 deaths in 2006 in the United States. The incidence and mortality of colorectal cancer has been decreasing in past two decades [7]. This decrease may result from improvement in the treatment and early detection.

Epidemiologic studies indicate that dietary and lifestyle factors play important roles in the risk of colon cancer [8]. The difference of colon cancer incidence between developed and developing countries is consistently correlated to the different environmental exposure. Physical inactivity, excess body weight, and a central deposition of adiposity have a major influence on the risk of colon cancer. Dietary constituents such as alcohol and meats may enhance the risk of colon cancer, while fiber from fruit and vegetables may reduce the risk. The incidence of colon cancer is high in western countries, where the diet contains more meats, fats, and refined carbohydrates but less vegetables. Recent evidence indicates that consumption of certain vitamins (D, A, C and E) could decrease the risk of colon cancer. Studies suggested that nonsteroidal

antiflammatory drugs (NSAIDs, e.g. aspirin) and postmenopausal estrogens may possibly reduce the colon cancer risk [9]. The migrant study implied that after immigration from a low-risk area (e.g. Japan) to a high-risk area (e.g. U.S.A.), the incidence of colon cancer increases rapidly within the first generation of migrants. The risk of Japanese born in the U.S.A. is nearly double that of their U.S. white neighbors [10].

1.2.2 Carcinogenesis of colon cancer

Approximate 90% of colon cancer is sporadic without known predisposing factors, while Familial adenomatous polyposis (FAP), the polyposis syndromes and hereditary non-polyposis colorectal cancer (HNPCC) account for about 5% of all colorectal cancers [11]. Most human colon adenocarcinomas evolved from aberrant crypt foci (ACF) and adenoma. Vogelstein *et al*. observed the development of colon cancer from small adenomas to large metastatic carcinomas and described the adenoma-carcinoma sequences as the stepwise progression from normal epithelium to adenoma to carcinoma associated with the accumulation of a number of genetic alterations (Figure 1.1) [12,13].

Molecular studies of colon adenoma and carcinoma have led to a genetic model of colon carcinogenesis (Figure 1.1). Mutations of APC (Adenomatous Polyposis coli), a tumor suppressor gene locates on chromosome 5q, initiate the neoplastic process,

resulting in hyperproliferative epithelium, and both alleles of the APC gene must carry an inactivating mutation in order to loss function. DNA hypomethylation is responsible for the conversion of hyperproliferative epithelium to early adenomas. The hypomethylation of DNA has been shown to inhibit chromosome condensation and might lead to mitotic nondisjunction, resulting in the loss or gain of chromosomes. The presence of *ras* gene mutation (e.g. K-*ras*), usually occurring in one of these benign tumor cells, contributes to a large and more dysplastic tumor through clonal expansion. Sequential mutations in the gene deleted in colon carcinoma (DCC) and p53 tumor suppressor genes appear to complete the process, resulting in progression from the benign to the malignant state [12,13].

1.3 Introduction to Dibenzoylmethane (DBM)

1.3.1 Chemical properties and metabolism of DBM

Dibenzoylmethane (DBM, 1,3-diphenyl-propanedion) has been found as the minor constituent of licorice (*Glycyrrhiza glabra* in the family of *Leguminoase*) and is classified as a rare kind of flavonoid [14]. Licorice is a traditional herb widely used as an antidote, demulcent and elixir folk medicine in China for thousands of years. It is also a food sweetening and flavoring agent used in the food industry.

As shown in Figure 1.2, DBM is a β-diketone compound with a molecular weight of 224.25 and a melting point of 76-78°C The maximum light absorption of DBM dissolved in acetonitrile in ultraviolet-visible spectrum occurs at 335nm. DBM has similar chemical structure with curcumin (diferuloylmethane), a yellow pigment from turmeric spices (Figure 1.2). Both DBM and curcumin contain a central β-diketone group in conjugation with an unsaturated carbon system, which may play a significant role in inducing Phase II enzymes [15]. Compared to curcumin, DBM lacks the phenolic hydroxyl groups and the reducible unsaturated alkyl groups. This may explain that why DBM shows a little or no antioxidant ability *in vitro* and is much better absorbed and distributed in tissue *in vivo* [16,17].

The metabolism of DBM in mice liver microsome has been recently reported (Lin, Chuan-Chuan; Ho, Chi-tang, Journal of food and drug analysis, 2005, 284). Only Chaconne was found in *in vitro* metabolism studies of DBM. Furthermore, the in vivo study in rats suggested mono- and di- hydroxylation flowed by Phase II conjugation was the major metabolic pathway of DBM. Based on *in vivo* study, monohydroxyl DBM is the major metabolite and then, conjugated by sulfation and glucuronidation. Interestingly, the monohydroxyl DBM could be further hydroxylated on the same aromatic ring to form dihyroxylated DBM. Similarly, dihyroxylated DBM are further metabolized to form

conjugates of single sulfation and glucuronidation [18] (Figure 1.3).

1.3.2 Biological activities of DBM

Inhibition of DMBA- or estradiol-induced mammary tumorigenesis by DBM

Breast cancer is the first leading cause in cancer-related deaths in women in the world in 2002 [6] and the second most common cause of cancer deaths among American women in 2006 [7]. DBM has been shown to inhibit 7, 12-dimethylbenz[a]antrance (DMBA)- or estradiol (E_2)-induced carcinogenesis of mammary gland both *in vivo* and *in vitro*[16,17,19-21]. DMBA is one of the known carcinogens that induce skin cancer or mammary tumor. DMBA interacts with the rapidly proliferating cells in the terminal end buds, forming DNA adducts, which in turn participate in transforming the normal terminal end bud cells to malignant pathways [22]. The dietary DBM inhibited *in vivo* mammary DMBA-DNA adduct formation and DMBA-induced mammary tumorigenesis in rats and mice, and also lowered the proliferation rate of the mammary gland *in vivo* [17,20,21]. DBM has been shown to dose-dependently inhibit DMBA metabolism and the formation of DMBA-DNA adducts, and this is considered as a potential mechanism accounting for the inhibition of DMBA-induced mammary tumor by DBM [16]. C. C. Lin *et al.* proposed two possible mechanisms for how DBM inhibits the formation of

DMBA-DNA adducts. One is that the influence of DBM on the metabolism of DMBA through Phase I and/or Phase II metabolizing enzyme systems, which would cause the reduction of bioactivated DMBA. The other one is that the inhibitory effect of DBM on the proliferation rate of mammary gland via the hormonal mitogenic pathway [20].

Some studies suggested that the risk of breast cancer rises with the increasing of endogenous estradiol (E_2) levels [23,24] Estradiol-induced over expression of oncogenes has been indicated to lead to the mammary tumorigenesis in animal and human cancer models [25,26]. The effect of DBM on E_2-induced mammary tumor has been studied in both human breast cancer cells and mouse mammary glands. In MCF-7 human breast cancer cells, DBM inhibited E_2-induced proliferation through the reduction of expression of the E_2-ER-ERE-dependent oncogenes, telomerase, *c-Myc*, *ha-ras*, and *bcl-2*. In a mouse model, DBM also inhibited the E_2-induced mammary gland proliferation. Further *in vivo* study suggested that DBM may act as a pure antagonist and reduce the binding of estrogen receptor to the estrogen response elements in the regulatory regions of *c-Myc*, *hTERT*, and *bcl-2* genes [19].

Regulation of Phase I and II enzymes by DBM

Phase I enzymes primarily consist of cytochrome P450 (CYP) family of

mixed-function oxidases and catalyze the reactions characterized by oxidative metabolism, resulting in the formation of either more polar or more electrophilic products [27]. The expression of some Phase I enzymes, e.g. CYP1A1, CYP1A2, and CYP1B1, is regulated by the AhR. It has been suggested that DBM is a natural ligand of AhR. DBM can inhibit AhR activation induced by carcinogens 7,12-dimethylbenz[a]anthracene (DMBA) or 2,3,5,7-tetrachlorodibenzo-p-dioxin (TCDD) by competing binding to AhR [28].

The induction of Phase II enzymes has been considered as one of the major strategies to prevent chemical-mediated cancers because these enzymes can detoxify carcinogens thus protect tissues against carcinogenesis [29] In hepa1c1c7 cells, DBM showed the capacity to induce quinone-reductase (QR) activity [21]. When fed to female rats, 1% DBM diet effectively blocked the initiation of DMBA-induced mammary tumorigenesis and inhibited mammary DMBA-DNA adducts formation. It was found that not only Phase II enzymes GST and QR, but also the Phase I enzyme EROD were induced by consumption of 1% DBM diet [21].

Effect of DBM on prostate cancer and skin cancer

DBM has been found to inhibit cell growth and to induce cell cycle arrest in LNCaP,

DU145, and PC-3 prostate cancer cells [30] and to suppress androgen receptor expression [31]. Exposure to 50 μM DBM for 72 hr caused cell cycle arrest in the G_0/G_1 Phase in LNCaP and DU145 cells, while S Phase arrest was observed in PC-3 cells. Interestingly, no significant increase in sub G_1 Phase was observed in flow cytometry analysis and no evidence of apoptosis was obtained by morphologic assessment.

It is widely accepted that the ultraviolet (UV) radiation plays a major role in skin tumor initiation and development because the most critical cellular target, DNA, can be damaged. DBM has also been used as a sunscreen to prevent the injurious effects of overexposure to solar radiation. Topical application of DBM to mouse skin inhibited both TPA-induced skin inflammation and TPA-induced skin tumor promotion in a dose dependent manner [17].

1.4 Summary

Colon cancer is one major public health problem in developed countries and the second leading cause of cancer-related deaths in the United States. DBM has been identified to suppress some cancers such as breast cancer. The mechanisms that modulated by DBM include the induction of Phase I & II enzymes, cell cycle arrest, apoptosis. In this thesis, the anti-carcinogenesis activity of DBM in HT-29 human colon

carcinoma cells and its pharmacokinetic disposition in the rats were studied. In Chapter 2, we observed that DBM inhibited the proliferation of and induced G_1 cell cycle arrest in HT-29 cells, and further studied the underlying molecular mechanism. Our results suggested that DBM induced G_1 cell cycle arrest by down-regulating the expression of Cyclin D1 and c-Myc and the phosphorylation of Rb protein in a p53-independent manner. In Chapter 3, I developed and validated a sensitive HPLC assay which is able to detect DBM in rat plasma, and further studied the pharmacokinetic disposition of DBM in rats. This study determined the pharmacokinetic profiles of DBM in the rats after intravenous or oral administration of the various doses. Together, this thesis will contribute to better understanding the molecular mechanism of cancer chemoprevention by dibenzoylmethane and the pharmacokinetic disposition of dibenzoylmethane in the rats.

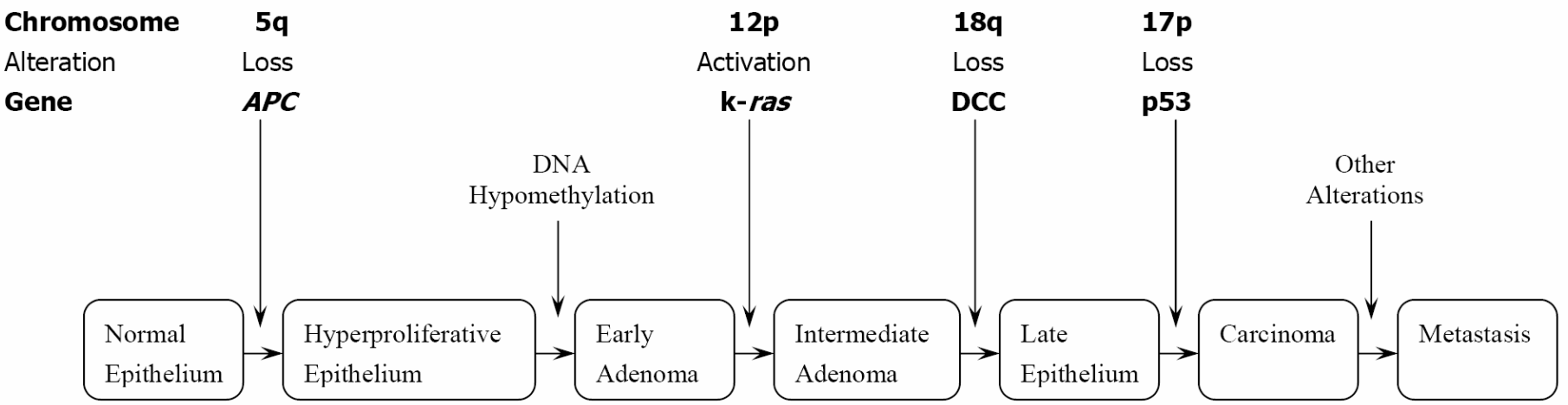

Figure 1.1 A genetic model for colorectal tumorigenesis. Modified form Ref. 9 .

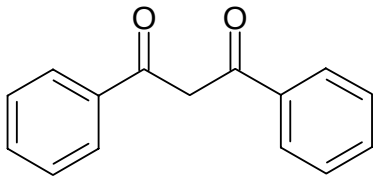

Dibenzoylmethane (DBM)

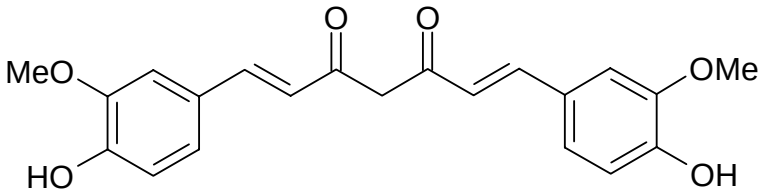

Diferuloylmethane (Curcumin)

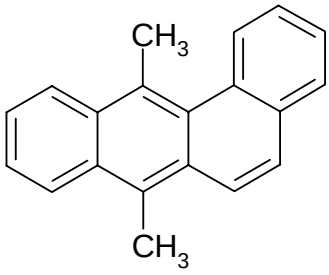

7,12-Dimethylbenz[a]anthracene (DMBA)

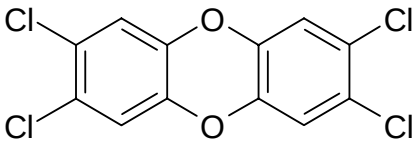

2,3,7,8-Tetrachlorodibenzo-*p*-dioxin (TCDD)

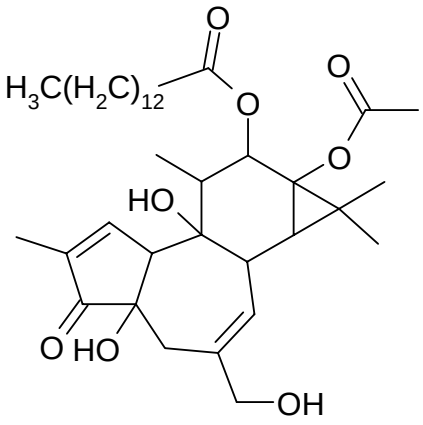

12-O-Tetradecanoylphorbol 13-acetate (TPA)

Figure 1.2 The structures of DBM, Curcumin, DMBA, TCDD and TPA.

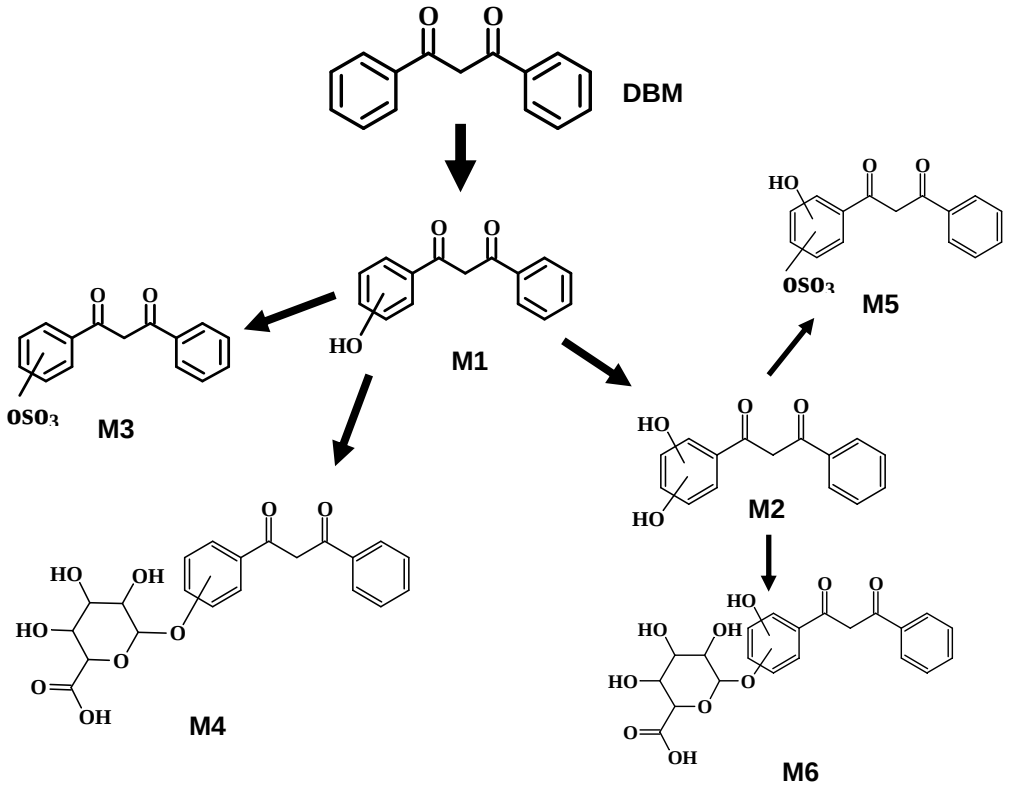

Figure 1.3 Proposed major metabolic pathways of DBM in C57BL/6J mouse. Ref.[18]

CHAPTER 2

Dibenzoylmethane induces cell cycle arrest by down-regulating Cyclin D1 and c-Myc in HT-29 human colon cancer cells

2.1 Introduction

The eukaryotic cell cycle is divided into four Phases: M (mitosis), G_1 (the period between mitosis and the initiation of nuclear DNA replication), S (the period of nuclear DNA replication), and G_2 (the period between the completion of nuclear DNA replication and mitosis) [32]. The major regulatory events leading to proliferation occur in the G_1 Phase. The time late in G_1 Phase was designated as the restriction point by Pardee, at which cells become committed to replicating DNA and divide or alternatively to exiting the cell cycle into a quiescent state (G_0) [33]. When stimulated by growth factor, these quiescent cells could re-enter the cell cycle. Once cells passed the restriction point, they irreversibly enter the S Phase and complete S, G_2 and mitosis in the absence of growth factors.

The cell cycle progress is governed by specific enzymes called the cyclin–dependent kinases (CDKs). As cells proceed through the cell cycle, four major cyclins are produced sequentially (D, E, A, and B), and these cyclins activate corresponding CDKs

[34]. The restriction point is controlled by the retinoblastoma protein (Rb)-E2F pathway, which is regulated by cyclin D- and cyclin E-dependent kinases [35]. The three D-type cyclins (D1, D2, and D3) interact with their catalytic partners (CDK4 and CDK6) to form at least six possible holoenzymes. The cyclin D/CDK4 and cyclin D/CDK6 complexes phosphorylate the retinoblastoma (Rb) protein on serine and threonine residues in mid-G_1 Phase [36]. Phosphorylation of Rb prevents its binding to E2F and results in the release of active E2F which activates the expression of genes whose products are necessary for nucleotide metabolism and DNA synthesis [37]. E2F also induces the expression of *cyclin E* and *A* genes that are required for entry into S Phase. Once Cyclin E is induced in late-G_1 Phase, the cyclin E/CDK2 complex collaborates with cyclin D/CDK to facilitate Rb phosphorylating and E2F releasing [38,39]. As cells approach G_1/S transition, the transcription of *cyclin A* gene is activated by high level E2F. Cyclin A/CDK2 complex is then assembled to trigger the initiation of DNA synthesis in S Phase. Cyclin B is firstly synthesized in the late-S Phase and accumulated as cells proceed through G_2 Phase. CDK1 is essential for mitosis Phase and its complexes to Cyclin A/B induce the event of mitosis [40,41].

Inhibitory proteins called CDK inhibitor (CDKI) further modulate the activity of the cyclin/CDK complexes. Two distinct families of CDK inhibitors, INK4s and CIP/KIPs,

have been described to modulate cell cycle. The INK4 (inhibitors of kinase 4) family members (p15, p16, p18, p19) directly bind to CDK4/6 and block their interaction with cyclin D in mid-G1 Phase [42]. This specific inhibitory effect results in decreased phosphrylation of Rb protein and prevents the transcriptional activation by E2Fs and the entry into the S Phase. The second class of CDKI is CIP/KIP family, including $p21^{CIP1}$, $p27^{KIP1}$ and $p57^{KIP2}$. These CIP/KIPs strongly inhibit the activity of the CDK2 complexes. In addition, phosphorylation of CDKs on specific threonine residue is required to activate CDKs. The activating phosphorylation of CDKs is catalyzed by CDK-activating kinase (CAK). Moreover, dephosphorylation of specific serines and tyrosines by the CDC25 phosphoatase is also necessary for activation of CDK [43,44].

c-Myc is a transcriptional regulator and play a role in G_1/S transition. It has been reported that ectopic c-Myc expression induces quiescent fibroblasts to enter cell cycle, reduces G1 duration, and promotes S Phase entry; conversely, down-regulation of c-Myc expression through antisense approach has antiproliferative effect [45]. c-Myc may affect cell cycle progression through modulating cyclin/CDK complexes, directly down-regulating the CDKI p27 and p21, and by interfering with Rb/E2F activity. c-Myc is destroyed via the ubiquitin/26S proteasome pathway [46].

Ubiquitin-proteasome proteolysis is the main pathway for the degradation of cell

cycle regulatory proteins [47]. Ubiquitin is a small 8-kDa protein and proteasomes are large cylindrical complexes which contain multiple proteases. The ubiquitin-proteasome proteolytic pathway involves two steps: the target proteins are marked by covalent addition of multiple ubiquitin molecules and rapid degradation by the 26S proteasome complex. The ubiquitination is a three-step process. The first step is activation of ubiquitin-activating enzyme by the addition of an ubiquitin molecule in an ATP-dependent manner. This activated ubiquitin molecular is transferred to a cysteine residue in ubiquitin-conjugating enzyme. Then, the ubiquitin is attached to the target protein by formation of a peptide bond, which is catalyzed by ubiquitin ligase resulting the polyubiquitin chain [32]. Finally, the ubiquitin-tagged proteins are recognized by 26S proteasomes and degraded in an ATP-dependent manner.

DBM has been shown to inhibit cell proliferation in colon cancer cells and induce cell cycle arrest in prostate cell lines. DBM also effectively inhibited cell proliferation in human colon cancer cells, COLO 205, by causing caspase-mediated apoptosis. In the current study, the effects of DBM on HT-29 human colon cancer cells were investigated. DBM dose-dependently inhibited HT-29 proliferation, mainly by cell cycle arrest. DBM induced cell cycle arrest in G_0/G_1 Phase by down-regulating the phosphorylation of Rb protein and the protein levels of several key G_1 regulatory proteins such as c-Myc and

Cyclin D1, possibly through proteasome-related pathway, and by up-regulating the CDK inhibitor protein p21. On the other hand, DBM exhibited no significant effect on cell apoptosis, as visualized by flow cytometry analysis and nucleosomal DNA ladders. In consistent with this, the protein level of p53 was not up-regulated by DBM.

2.2 Material and Method

Materials

DBM (purity: 98%) was purchased from Sigma (St. Louis, MO, USA) and dissolved in DMSO. MG132, a proteasome inhibitor, was from Calbiochem (San Diego, USA). Antibodies against p21, Cyclin D1 and Actin were obtained from Santa Cruz Biotechnology (Santa Cruz, USA). Antibodies against phosphor-Rb and c-Myc were from Cell Signaling (Danvers, MA). All cell culture products were obtained from Invitrogen (Carlsbad, CA). TRIzol and SuperScript First-strand Synthesis System for RT-PCR are also purchased from Invitrogen (Carlsbad, CA). The primers used for RT-PCR are from Integrated DNA Technologies (Coralville, IA).

Cell Culture

The human colorectal cancer cells, HT-29, were obtained from American Type Culture

Collection (ATCC, Manassas, VA, USA), and were maintained in the complete Minimum Essential Medium (MEM) supplemented with 10% Fetal Bovine Serum (FBS) and 1% penicillin/streptomycin and kept in a humidified incubator of 5% CO_2 at 37^{o}C.

Cell Proliferation assay

Cell Proliferation was measured by MTS Assay. HT-29 cells were cultured in 96-well plates at a density of 2500 cells/well. After 24 hr, cells were serum starved for 36 hr. Then, the culture medium was replaced with fresh MEM containing 10% FBS and DBM at different concentrations and the cells were cultured for further 24 or 48 hr. DMSO was added to controls with a final concentration of 0.1%. Cell viability was determined by using the Cell Titer non-radioactive cell proliferation assay kit (Promega, Madison, WI) according to the protocol provided by the manufacturer. The percentage of viable cells was calculated as a ratio of A_{490nm} of treated cells versus control cells.

Cell Cycle Analysis

HT-29 cells were seeded in 60-mm dishes at a density of 10^5 cells/dish and allowed to attach overnight. The cells were starved in serum free MEM for 36 hr. Then, the medium was replaced with fresh complete MEM containing desired concentration of DBM. After

24 hr, both floating and adherent cells were harvested, washed in ice-cold PBS, and fixed in 70% ethanol. The fixed cells were collected by centrifugation and resuspended in 500 μL PBS containing 100 μg/mL RNase A and 10 μg/mL propdium iodide on ice for 30 min. The cell cycle distribution was then analyzed by flow cytometry using Coulter Cytomics FC500 Flow Cytometer (Fullerton, CA).

Western Blotting

Cells (5×10^4 cells/well) were plated in 6-well plate and incubated for 24 hr followed by 36 hr serum starvation; then the cells were treated with either DBM or DMSO as described. The cells were washed by ice-cold PBS, and lysed with MAPK lyses buffer (10 mM Tris-HCl, pH 7.9, 50 mM NaCl, 30 mM sodium pyrophosphate, 50 mM sodium fluoride, 0.5% Triton X-100, 1X proteinase inhibitor mixture, 1 mM phenylmethylsulfonyl fluorid, 100 μM Na_3VO_4, 5 μM $ZnCl_2$, 2 mM indole acetic acid). The cell lysates were centrifuged at 4 ℃, 13000 rpm for 5 min. The protein concentration was determined by protein assay kit (Pierce, Rockford, IL). 20 μg of total cellular proteins were resolved by 8-15% SDS-PAGE and electro-transferred onto a polyvinylidene fluoride (PVDF) membrane. The membrane was blocked in 5% Bovine Serum Albumin for 1 hr at room temperature, then incubated with desired primary

antibodies at 4℃ overnight. The membrane was washed with TBST (20 mM Tris-HCl, 8 g/L NaCl, 0.1% Tween 20, pH 7.6) three times, then incubated with appropriate HRP-conjugated secondary antibody for 1 hr at room temperature followed by three washes with TBST. The bound antibodies were then visualized by SuperSignal® West Femto Maximum Sensitivity Substrate (Pierce, Rockford, IL) using a Bio-Rad ChemiDoc XRS system (Hercules, CA)

Reverse Transcriptase PCR

After starvation, cells were treated with DBM as described above. The total RNA was extracted by using TRIzol reagent (Invitrogen, Carlsbad, CA) following the manufacturer's protocol and cDNA was then synthesized from 5 μg of total RNA using SuperScript First-strand Synthesis System for RT-PCR (Invitrogen, Carlsbad, CA) according to the manufacturer's protocol. PCR reaction was performed by using 2 μL of cDNA product, 2 μL of primer mixture (final concentration 10uM) and 6 μL of PCR SuperMix (Invitrogent, Carlsbad, CA), and conducted for 30-35 cycles in Peltier Thermal Cycler (Bio-Rad, Hercules, CA). Primers and cycles used for amplification are listed in Table 2.1. Each amplification cycle consisted of 1 min at 94℃ for denaturation, 0.5 min at 55℃ for primer annealing, and 1 min at 72℃ for extension. After PCR amplification,

the products were analyzed by agarose gel electrophoresis and visualized using ethidium bromide staining.

MG132 Treatment

Cells (5×10^4 cells/well) were plated in 6-well plate and serum starved as described. The cells were pretreated with either DMSO or 10 mM MG132 for 30 min and then exposed to DBM for 1 hr or 4 hr in the absence or presence of MG132. The cells were then harvested and subjected to western blotting as described above.

Statistical Analysis

All values are presented as the mean ± SD of the mean. All experiments were repeated at least three times. The statistical significance was evaluated using the paired Student's t-test for comparison between two means. P values < 0.05 were considered to be statistically significant.

2.3 Result

2.3.1 DBM inhibited cell proliferation in HT-29 cells.

We first examined the growth inhibitory effect of DBM on the human colon cancer cell line, HT-29. As shown in Figure 2.1, DBM inhibited cell proliferation in HT-29 cells in a concentration-dependent manner and in a very similar pattern at 24 hr and 48 hr. The proliferation of HT-29 cells stimulated by serum was significantly inhibited by 75 and 100 μM of DBM. Treatment with 100 μM DBM caused a decrease of 35% in cell proliferation at 24 hr, and 45% at 48 hr, compared to the DMSO-treated controls. These results indicate that DBM inhibits the serum-stimulated proliferation of HT-29 cells.

2.3.2 DBM induced G1 Phase cell cycle arrest in HT-29 cells.

HT-29 cells were incubated in serum free MEM for 36 hr to synchronize cells in G_0/G_1 Phase. Then, the medium was replaced by 10% Serum-supplemented medium with 0.1% DMSO (as control) or DBM at indicated concentrations for 24 hr. The effect of DBM on cell cycle distribution was determined using flow cytometry analysis (Figure 2.2). The results showed that DBM induced G_0/G_1 arrest of HT-29 cells in dose-dependent manner. The percentage of cells in G_0/G_1 Phase increased from 52.18%

in the DMSO-treated control cells to 78.44% in the cells exposure to 100 μM DBM after 24 hr. Concomitantly, the percentage of cells in S and G_2/M Phases decreased. However, only very low sub-G_1 cells were observed even after exposure to 100 μM DBM for 24 hr. This data suggests that DBM significantly induced HT-29 cells arrest in G_0/G_1 Phase but has little effect on cell apoptosis.

2.3.3 DBM did not induce apoptosis in HT-29 cells

According to very low sub-G_1 cells observed by flow cytometry, the effect of DBM on p53 level and DNA fragmentation HT-29 cells was examined. As shown in Figure 2.3, the level of p53 protein was not up-regulated after 24 hr of DBM treatment. In addition, nucleosomal DNA ladders showed no DNA fragmentation induced after 24 or 48 treatment of 100 μM DBM (Data not shown). These results are consistent with the observation from the flow cytometry analysis, suggesting DBM did not induced apoptosis in HT-29 cells.

2.3.4 DBM modulated the expression of G_1 cell cycle regulatory proteins

Because DBM induced a G_0/G_1 arrest in HT-29 cells, we next examined the effects of DBM on several key G_1 Phase regulatory proteins, such as phosphor-Rb, c-Myc,

Cyclin D1 and $p21^{CIP1}$ using western blotting. As shown in Figure 2.4, upon DBM treatment, the level of phosphor-Rb, Cyclin D1 and c-Myc markedly decreased in a dose-dependent manner after 1 hr, while the level of p21 was induced at 24 hr but not 1 hr. The changes in protein expression induced by DBM are consistent with the above-described G_1 cell cycle arrest.

2.3.5 DBM affected the expression of cell cycle regulatory genes

We next use semi-quantitative RT-PCR to determine the effects of DBM on the expression of c-Myc, Cyclin D1 and p21. HT-29 cells were starved for 36 hr and treated with DBM at varying concentration for 24 hr. PCR reaction was performed as described in "Material and Method" and the results were shown in Figure 2.5. After treated with DBM for 24 hr, the transcription of c-Myc and Cyclin D1 was down-regulated in dose-dependent manner, whereas $p21^{CIP1}$ was up-regulated. These results are consistent with western blotting results.

2.3.6 Proteasome-mediated degradation was involved in DBM-mediated down-regulation of Cyclin D1 and c-Myc

We investigated whether the down-regulation of Cyclin D1 and c-Myc induced by

DBM involved the proteasome-mediated signal pathway. The effect of the specific proteasome inhibitor, MG132, on the DBM-induced decline in Cyclin D1 and c-Myc protein level was studied. After 36 hr serum starvation, HT-29 cells were pretreated with10 μM MG132 or DMSO (as control) for 30 min in the fresh MEM with 10% FBS and then, treated with DMSO or 100 μM DBM in the absence or presence of 10 μM MG132 for 1 or 4 hr. As Figure 2.6 shown, DBM-induced decrease of Cyclin D1 and c-Myc was almost completely blocked by MG132. These data indicated that DBM down-regulated Cyclin D1 and c-Myc by proteasome-mediated pathway.

2.4 Discussion

DBM has been found to inhibit cell proliferation and show potent cancer chemopreventive effect in rat models of mammary tumorigenesis [48]. In addition, DBM suppressed cell growth and caused cell cycle arrest in the prostate cancer cell lines [30], and also inhibited cell proliferation in human colon cancer cells, COLO 205 [49]. Previous work in our lab showed that DBM effectively inhibited familial adenomatous polyposis in Apc(Min/+) mice [48]; however, the cellular and molecular mechanisms underlying the inhibition remained unclear. In this study, we tested the effect of DBM on the growth of human colon cancer cells, HT-29, and further investigated the possible

molecular mechanisms.

The results of MTS assay for the first time showed that DBM inhibited the cell growth on HT-29 cells (Figure 2.1). Since the inhibition of cell growth could be resulted from decreased proliferation or increased cell death, we further checked the effect of DBM on the cell cycle distribution and apoptosis of HT-29 cells. As shown in Figure 2.2, DBM induced cell cycle arrest in G_0/G_1 Phase in the dose-dependent manner in HT-29 cells. Moreover, we demonstrated that this arrest was associated with modulation of cell cycle regulatory pathways such as c-Myc, Cyclins D1, and Rb pathways. After synchronizing cells in G_0 Phase, treatment of 100 μM DBM for 24 hr caused 78.44% cells arrested at G_0/G_1 Phase, while 52.18% control cells retained in G_0/G_1 Phase. On the contrary, no significant increase of cell apoptosis was detected by either nucleosomal DNA ladder or the sub-G_1 peak in flow cytometry analysis (Figure 2.2). Taken together, these data suggested that DBM inhibited the cell growth of HT-29 cells mainly by inhibition of cell cycle progression rather than induction of cell apoptosis.

As mentioned in “Introduction”, cyclin D/CDK4 and cyclin E/CDK2 complexes control the progression of cell cycle from the G_1 to the S Phase. These complexes will activate Rb pathway via phosphorylating Rb and thus transcriptionally activate E2F target genes to trigger G_1-S transition. Several serine and threonine phosphorylation sites on

Rb protein are crucial for the regulation of the G_1/S trasition, and Ser795 and ser807/811 have been reported to be the phosphorylation sites for CDK4/Cyclin D1 [50]. As expected, DBM rapidly decreased the levels of Cyclin D1 and phosphor-Rb after 1 hr and 24 hr of DBM treatment on HT-29 cells (Figure 2.4). Accordingly, the phosphorylation of Rb at Ser795 and ser807/811 was also dose-dependently inhibited by DBM. Furthermore, we observed that DBM decrease the mRNA level of Cyclin D1 within 24 hr (Figure 2.5). These data suggest that the mechanism of DBM induced G_1 arrest is to suppress the expression of Cyclin D1 in association with dephosphoylation of Rb.

During the progression of cell cycle, the CDKI $p21^{CIP1}$ and $p27^{KIP1}$ often play important roles in regulation of cyclin/CDK complex activity. The induction of $p21^{CIP1}$, which may be regulated through p53-dependent or p53-independent manner, can result in cell cycle arrest in G_1 Phase. Our data showed that DBM up-regulated $p21^{CIP1}$ with 24 hr of treatment on HT-29 cells, but this upregulation was not observed within 1 hr of treatment (Figure 2.4). Consistently, DBM also induced the mRNA expression of $p21^{CIP1}$ with 24 hr of treatment (Figure 2.5). No significant change in the protein level of the cell cycle regulatory proteins p53 was observed (Figure 2.3). These results suggested that DBM might activate the transcription of the $p21^{CIP1}$ gene via a p53-independent mechanism.

c-Myc is another crucial regulator of cell cycle progression, especially during the transition from the G_1 to the S Phase. Down-regulation of c-Myc can lead to inhibition of the cyclin/CDK complexes and increased level of CDKI, and finally lead to cell cycle arrest at G_0/G_1 Phase. We found that DBM down-regulated both the protein and mRNA levels of c-Myc in HT-29 cells (Figure 2.4 and 2.5). The protein levels of these cell cycle regulatory proteins are often regulated by proteasome-mediated degradation. So we tested the effect of the 26S proteasome inhibitor MG132 on the protein levels of Cyclin D1 and c-Myc, and found that MG132 prevented the down-regulation of them (Figure 2.6).

In summary, our results indicate that DBM inhibits cell growth in HT-29 cells by inducing cell cycle arrest at G_0/G_1 Phase rather than inducing apoptosis. The molecular mechanism of DBM-induced cell cycle arrest involves the up-regulation of $p21^{CIP1}$ and down-regulation of Cyclin D1, c-Myc, and dephosphorylation of Rb via p53-independent pathways. The down-regulation of Cyclin D1 and c-Myc, were resulted from proteasome-mediated protein degradation and decreased mRNA transcription. These results suggest that DBM can act as a potent and safe chemopreventive agent.

Table 2.1 The primers are used for amplification in RT-PCR.

Primer	Orientation	Sequence	Ref
Cyclin D1	Sense	5’-AGC CAT GGA ACA CCA GCT CCT GTG-3’	[51]
	AntiSense	5′-GAT GGA GCC GTC GGT GTA GAT GCA-3′	
c-Myc	Sense	5′-CAA GAG GCG AAC ACA CAA CGT CT-3′	[51]
	AntiSense	5′-AAC TGT TCT CGT CGT TTC CGC AA-3′	
p21	Sense	5′-GTG AGC GAT GGA ACT TCG A-3′	[52]
	AntiSense	5′-AAT CTG TCA TGC TGG TCT GC-3′	
Actin	Sense	5′-CGT ACC ACT GGC ATC GTG AT-3′	[53]
	AntiSense	5′-CGT ACC ACT GGC ATC GTG AT-3′	

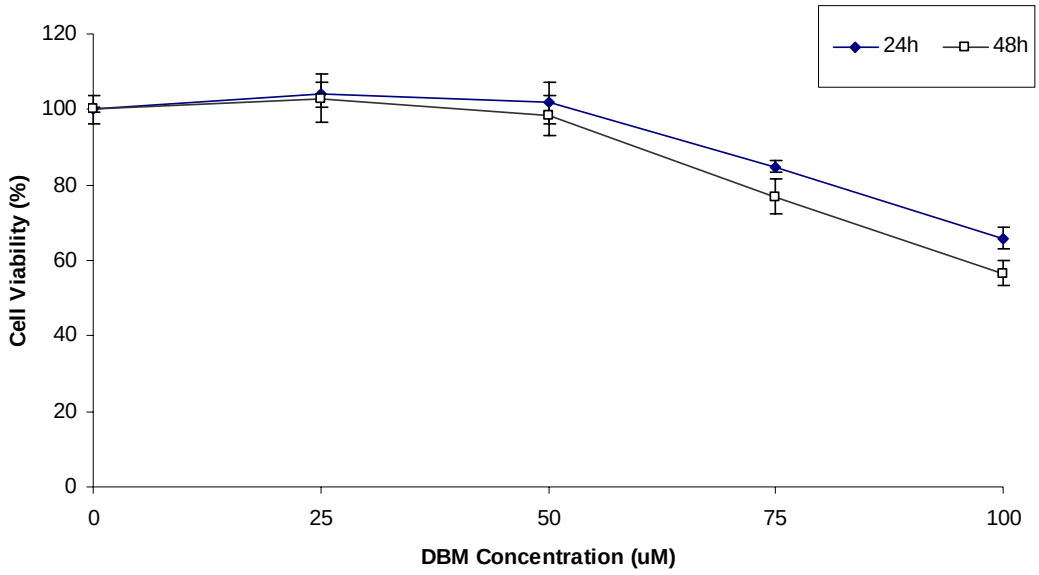

Figure 2.1 Effect of DBM on cell growth of HT-29 cells. Cells were seeded in 96-well plates at a density of 2500 cells/well. After 36 hr serum-starvation, cells were treated with increasing concentration of DBM for 24 or 48 hr. Cell viability was determined by MTS Assay. Data presented are mean ± SD of six replicates and are from one typical experiment among three experiments.

DBM (μM)	G0/G1	G2/M	S
0	42.89	27.06	30.05
25	44.25	23.57	32.18
50	58.84	16.89	24.27
75	65.5	11.96	22.54
100	67.37	14.59	18.04

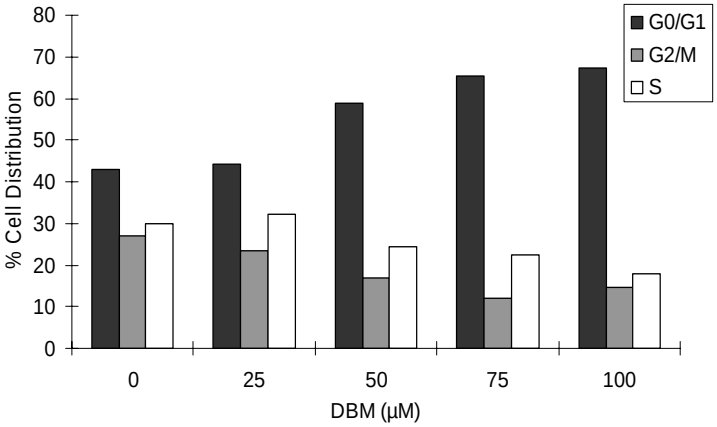

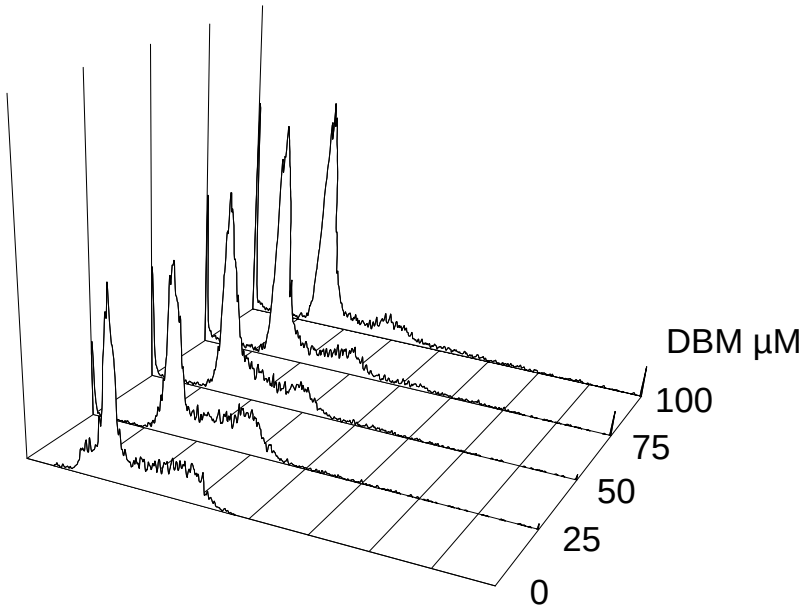

Figure 2.2 Effect of DBM on HT-29 cell cycle distribution. After synchronizing in G_0/G_1 Phase, cells were treated with DBM at the concentration of 0, 25, 50, 75, 100μM for 24 hr. Cell distribution was analyzed by flow cytometry as described in "Materials and Methods." Results are expressed as the percentage of total cells and are from one typical experiment among three experiments.

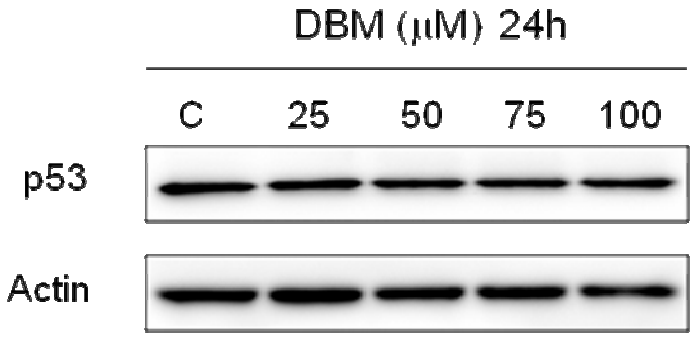

Figure 2.3 Effect of DBM on p53 protein level in HT-29 cells. HT-29 cells were grown in the plates for 24 hr and treated with varying concentration of DBM for 24 hr. Western Blot analysis for p53 and actin were performed.

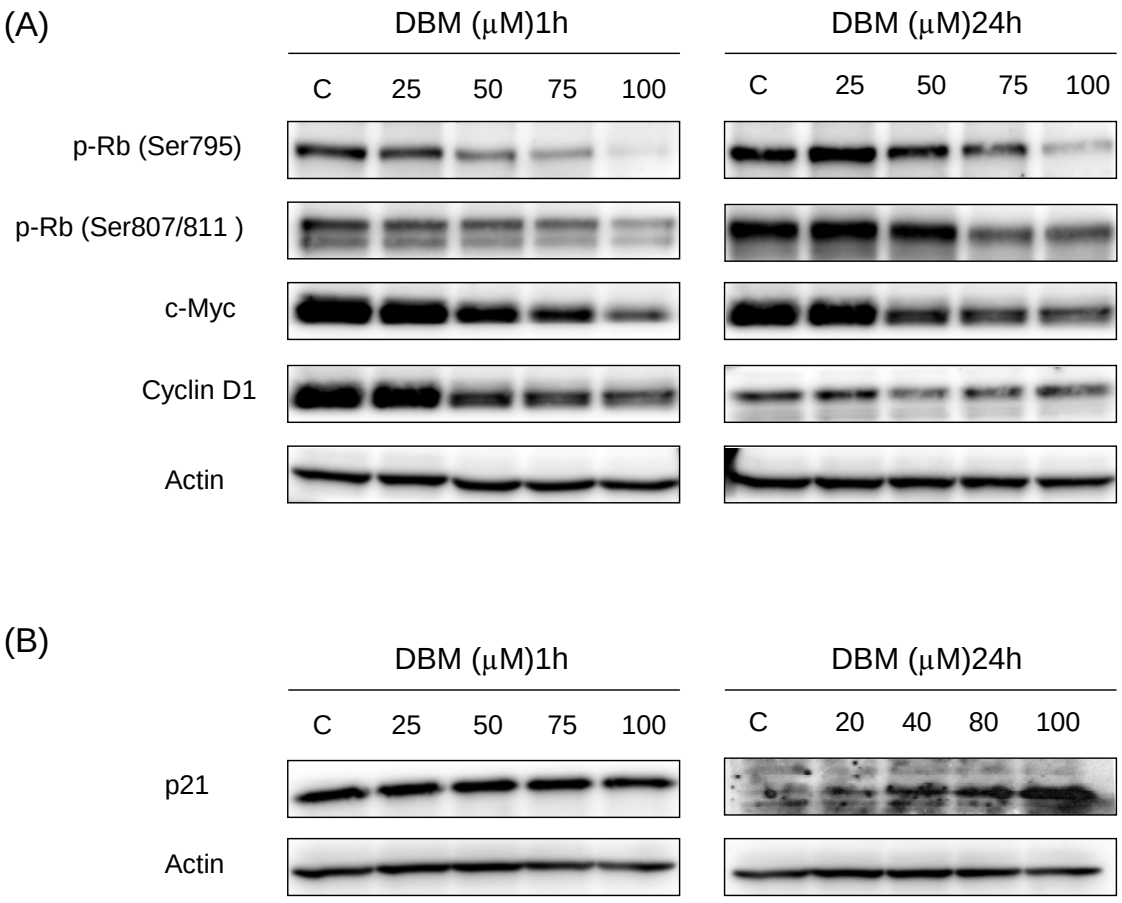

Figure 2.4 Effects of treating HT-29 cells with DBM on the various cell cycle regulatory proteins. HT-29 cells were treated with increasing concentration of DBM for 1 or 24 hr. Cell extracts were examined by Western Blot analysis as described in "Materials and Method." Actin was used as an internal control.

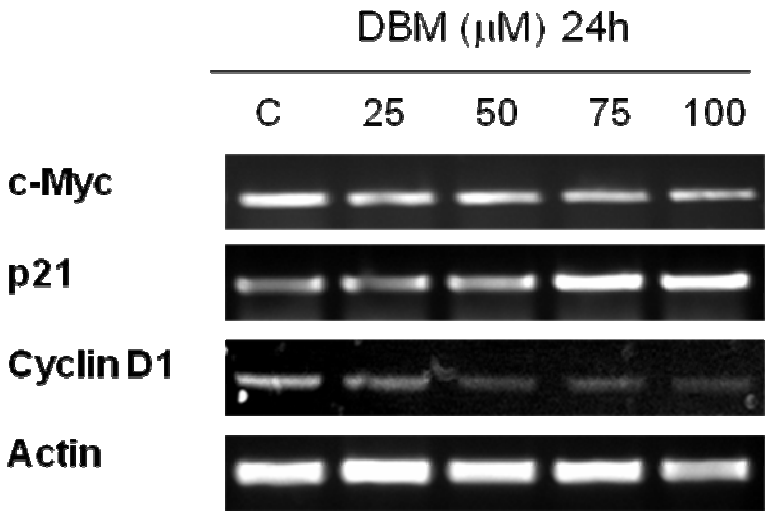

Figure 2.5 Effect of DBM on G_1 cell cycle regulatory gene expression. HT-29 cells were serum-starved for 36 hr and treated with different concentration of DBM for 24 hr. RNA was extracted and analyzed by RT-PCR as indicated in "Materials and Method." Actin was used as an internal control. RT-PCR are repeated at least twice.

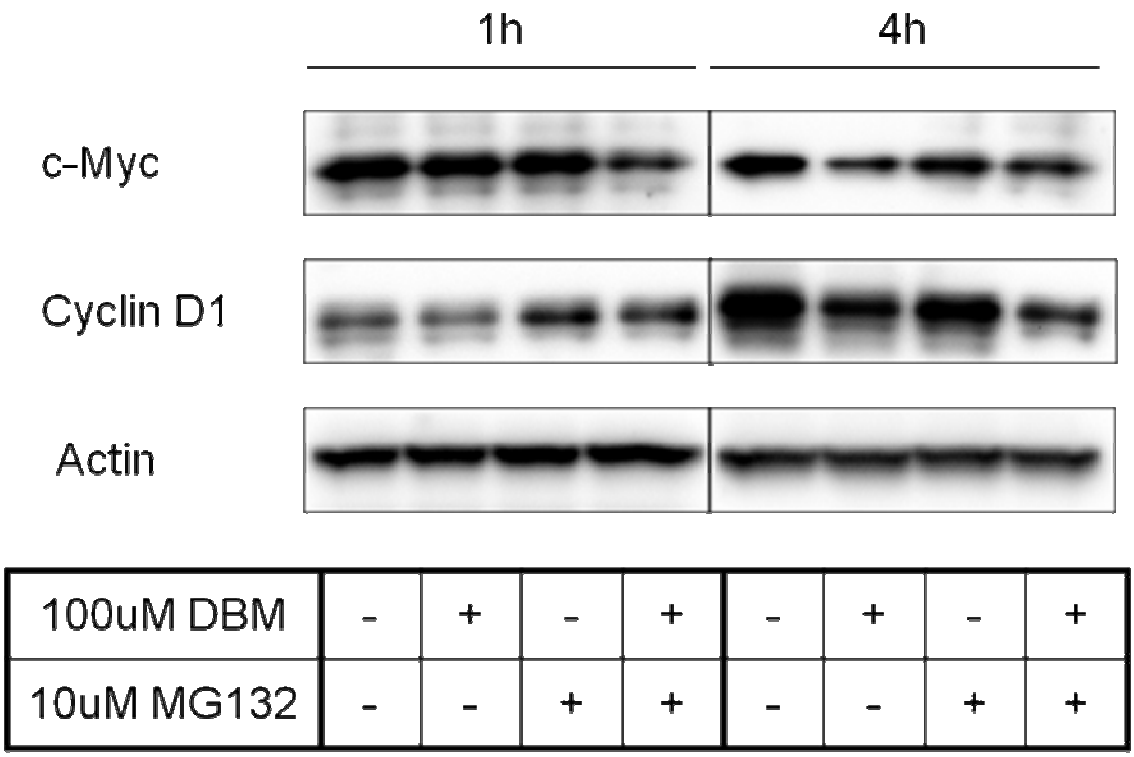

Figure 2.6 Effect of a proteasome inhibitor (MG132) on HT-29 cells. After 36hr serum-starvation, cells were pretreated with 10 μM MG132 or 0.1% DMSO (control) for 30 min and then, treated with 100 μM DBM in the absence or presence of 10 μM MG132 for 1 or 4 hr. Cell extracts were examined by Western Blot analysis as described in "Materials and Method." Actin was used as an internal control. Data shown are from one typical experiment among three experiments.

Chapter 3

Development and validation of an HPLC method for the determination of dibenzoylmethane (DBM) in rat plasma and its application to the pharmacokinetic study

3.1 Introduction

Many dietary compounds have been reported to possess anticarcinogensis ability *in vitro* and *in vivo*. These dietary compounds are isolated from either food source or plants, and thus, considered natural and safe to human. However, dietary compounds might have poor absorption, extensive metabolism and rapid clearance from body. These properties render them inactive in pharmacological effect, particularly after oral administration. For example, green tea polyphenols, particularly EGCG, are known for their chemopreventive potential in many types of cells and animal models [54]. EGCG and other polyphenols are poorly absorbed and undergo substantial biotransformation, leading the low pharmacological effect in clinical studies. The efficacy of EGCG in clinical studies was very low. Curcumin is also very potent in cancer chemoprevention, but its plasma concentrations were found to be very low in rodents and human after oral administration probably due to low bioavailability [18]. Therefore, for further clinical

application, the dietary chemopreventive compounds require more knowledge of *in vivo* pharmacokinetics including absorption, distribution, metabolism and excretion. Identification of pharmacokinetic properties of these chemopreventive agents is important to correlate to their pharmadynamic effect *in vivo* as well as the pharmacological efficacy in clinical studies.

To our knowledge, no analytical method has been developed and validated to measure the concentration of DBM in those previous studies, nor has the pharmacokinetics of DBM been investigated. Therefore, in this study, we reported the development and validation of a sensitive HPLC assay to quantify DBM in rat plasma, and the use of this assay to characterize the basic pharmacokinetic characteristics of DBM in male Sprague-Dawley rats.

3.2 Experimental methods

3.2.1 HPLC analysis

3.2.1.1 Chemicals and reagents

1,3-Diphenyl-1,3-propanedione (dibenzoylmethane, DBM,) and internal standard (I.S.) 1-(5-Chloro-2-hydroxy-4-methylphenyl)-3-phenyl-1,3-propanedione (CHMPP) were purchased from Sigma (St. Louis, MO, USA) at purity of more than 98%, their

chemical structures were illustrated in Figure 3.1. Acetonitrile and methanol were all HPLC grade from Fisher Scientific. Trifluoroacetic acid (TFA) was spectrophotometric grade (> 99%, Aldrich, WI, USA). Ethyl acetate was purchased from Sigma with purity of 99.9%. Other chemicals used in this study were all in analytical grade unless specified.

3.2.1.2 HPLC instruments and chromatographic conditions

The Shimadzu HPLC system (SCL-10A vp) consists a model FCV-10AL vp binary pump, a model SIL-10AD vp autosampler (a 250 μL injector with a 100 μL loop) conFigured with a 4°C cooler, and a model SPD-10AV vp UV-Vis detector. The column and autosampler temperatures were kept at room temperature and 4°C, respectively. The reverse Phase chromatography was performed with an analytical Gemini^{TM} C18 column (150 x 2.0 mm, 5-μm, Phenomenex, Torrance, CA USA) protected with a SecurityGuard^{TM} cartridge system (Phenomenex) and a 0.45-μm in-line filter. The optimized method used a binary gradient mobile Phase with water/methanol (80:20, v/v) containing 0.1% TFA as mobile Phase A and acetonitrile with 0.1% TFA as mobile Phase B, the time program of the gradient was listed in Table 3.1. The flow rate was 0.2 mL/min and the injection volume was 20 μL. The UV detector was set at a single wavelength of 335 nm. The Class-VP software version 7.1.1 (Shimadzu, MD USA) was used for

instrument control and data analysis.

3.2.1.3 Stock solutions and standards

Primary stock solutions of DBM (1 mg/mL) were prepared in methanol whereas stock solutions of internal standard CHMPP (1 mg/mL) were prepared in DMSO and stored at -80°C. Primary stock solution of DBM was firstly diluted quantitatively with methanol to give working solutions with concentrations of 0.5, 1.0, 2.5, 5.0, 10, 50, 100 and 200 μg/mL for the preparation of calibration and quality control (QC) samples. Internal standard CHMPP primary stock solution was diluted 5 times twice with DMSO to give a working solution at concentration of 40 μg/mL. DBM calibration standards were prepared fresh daily at concentrations of 0, 0.05, 0.1, 0.25, 0.5, 1.0, 5.0, 10 and 20 μg/ml by spiking 50 μL blank rat plasma with 5 μl of methanol (for “zero” standard sample) or DBM working solutions. Each standard sample was also spiked with 2.5 μL of internal standard CHMPP working solution to give a final concentration of 2 μg/mL. In the same manner, QC samples with 2 μg/mL CHMPP and concentration of DBM at low (0.05 μg/mL), medium (1.0 μg/mL), and high (20 μg/mL) were freshly prepared to evaluate accuracy and precision of this HPLC method.

3.2.1.4 Sample preparation procedures

A 50 μL blank rat plasma, spiked plasma or pharmacokinetics study plasma sample was extracted with 200 μL ethyl acetate/methanol (95:5 v/v) solution by mixing for 2 min on a cyclomix at room temperature, the upper layer was transferred to a clean tube after centrifugation at 10,000 g for 3 min. The extraction procedure was repeated once and the combined organic Phase was evaporated to dryness under a stream of nitrogen gas at room temperature. The obtained residue was reconstituted in 100 μL of acetonitrile/water (50:50 v/v) by vortexing for 2 min, filtered through a 0.45 μm Nylon Spin-filter (Analytical Sales, NJ) and transferred into a sample vial for HPLC analysis.

3.2.2 HPLC method validation

3.2.2.1 Specificity and selectivity

The chromatographic interference from endogenous compounds was assessed by comparing chromatograms of blank rat plasma, plasma spiked with DBM and internal standard CHMPP, and plasma samples obtained from DBM pharmacokinetic studies in the rats.

3.2.2.2 Sensitivity

The lower limit of quantification (LLOQ) was determined during the evaluation of the linear range of calibration curve. LLOQ was defined as the lowest concentration yielding a precision with CV less than 20% and accuracy within 15% of the theoretical value (i.e. accuracy between 85% and 115%) for both intra- and inter-day analysis.

3.2.2.3 Linearity of calibration curve

Calibration curve was obtained by plotting the peak area ratios of DBM/CHMPP to the spiked DBM theoretical concentrations in blank plasma. The linearity of calibration curve was evaluated by linear regression analysis. The minimally acceptable correlation coefficient (r^2) for the calibration curve was 0.99 or greater.

3.2.2.4 Precision and accuracy

In order to assess the intra- and inter-day precision and accuracy of the assay, DBM QC samples at low, medium and high concentrations were prepared as described above. The intra-day precision of the assay was assessed by calculating the coefficients of variation (CV) for the analysis of QC samples in three replicates; and inter-day precision was determined by the analysis of QC samples on three consecutive days. Accuracy was

calculated by comparing the averaged measurements and the nominal values and expressed in percent. The criteria for acceptability of precision were that the relative standard deviation (R.S.D.) for each concentration level should not exceed ± 15% with the exception of the LLOQ, for which it should not exceed ± 20%. Similarly, for accuracy, the averaged value should be within ± 15% of the nominal concentration except for the LLOQ, where the limit was ± 20%.

3.2.2.5 Recovery

The absolute extraction recovery of DBM was determined with QC samples by comparing peak area ratio of DBM/CHMPP to those of standards in acetonitrile at equivalent concentrations and expressed in percentage.

3.2.2.6 Stability

Stability of DBM in rat plasma at room temperature for 4 h was evaluated using QC samples in triplicates. Three freeze-thaw cycles (- 80°C/room temperature) were applied to QC samples to assess the stability of DBM. Freezing stability of DBM in rat plasma was assessed by analyzing QC samples stored at - 80°C for one month. The in-autosampler (4°C) stability of DBM in the reconstitute solvent was evaluated by

reinjecting QC samples 48 h after the initial injection. The peak area of DBM in different QC levels at initial condition was used as reference to determine the relative stability of DBM in the experiments described above.

3.2.3 Pharmacokinetics of DBM in the rats

3.2.3.1 Pharmacokinetic study of DBM

Male Sprague-Dawley rats with weight between 250-300 g and jugular vein cannulae were purchased from Hilltop Lab. Animals Inc. (Scottdale, PA USA). Rats were housed at Animal Care Facility of Rutgers University under 12 h light-dark cycles with free access to food and water. Upon arrival, rats were given AIN-76A diet (Research Diets, NJ USA) free of antioxidant and acclimatized for 3 days. Rats (n=3) were fasted overnight and given DBM at dose of 50 mg/kg in a vehicle of Cremophor EL/tween-80/ethanol/water (2:1:1:6 v/v) by oral gavages (p.o.). Rats (n=3) were also given DBM at dose of 10 mg/kg in the same vehicle as an intravenous (i.v.) bolus through the jugular vein cannulae. Blood samples (200 μL) were collected at 2 (i.v. only), 7.5, 15, 30 min, 1, 1.5, 2, 4, 6, 8, 12, 24, and 36 h following DBM administration. Plasma was separated immediately by centrifugation and stored at - 80°C until analysis.

3.2.3.2 Pharmacokinetic Analysis

The DBM plasma concentration data was analyzed by non-compartmental and compartmental analyses using WinNonlin 4.0 software (Pharsight, CA USA) to obtain the appropriate pharmacokinetic parameters. The area under the plasma concentration versus time curve (AUC_{0-t}) from time zero to the time of last measured concentration (Clast) was determined using the log-linear trapezoidal rule. The AUC zero to infinite ($AUC_{0-\infty}$) was obtained by the addition AUC_{0-t} and the extrapolated area calculated by Clast/kel. The elimination rate constant (*kel*) was estimated from the slope of terminal Phase and the half-life ($t_{1/2}$) was calculated using the equation $t_{1/2} = \ln 2/kel$. The mean residence time (MRT) was calculated as $AUMC_{0-\infty}/AUC_{0-\infty}$, where $AUMC_{0-\infty}$ is the area under the first moment versus time curve. Clearance (Cl) was estimated by $Dose/AUC_{0-\infty}$ for intravenous route. The volume of distribution at steady state (Vd_{SS}) was calculated as $Cl \times MRT_{IV}$. The maximum plasma concentration (C_{max}) and the time to reach the C_{max} were obtained directly from the plasma concentration-time profile. The absorption rate (*ka*) is calculated by equation: $MRT_{PO}\text{-}MRT_{IV} = 1/ka$. The absolute bioavailability (F) is determined by the ratio of the dose-normalized $AUC_{0-\infty}$ following oral and intravenous administration.

3.2.4 Statistical Analysis

Statistical analysis was conducted using a one-way ANOVA followed by Bonferroni's tes or using a Student's t test. Statistical significance was set at $p < 0.05$.

3.3 Results and discussion

3.3.1 Method development

The UV-Vis absorbance of DBM was scanned from wavelength of 200-800 nm on a Beckman DU530 UV-Vis spectrophotometer. As shown in Figure 3.2, DBM (25 μg/mL) has maximum UV absorption at wavelength of 335 nm in acetonitrile; therefore, wavelength of 335 nm was chosen for UV detection in this assay. Chromatograms of DBM standard (1 μg/mL acetonitrile) analyzed by reverse Phase HPLC analytical columns including Luna Phenyl-Hexyl, Gemini C18, Synergi Max-RP from Phenomenex (150 × 2.0 mm, 5-μm), Waters Xterra C18 and Shimadzu Premier C18 were compared. The Gemini C18 column was selected for the assay based on its given DBM retention time, peak shape/symmetry and selectivity (Data not shown). The mobile Phase used for the assay was of very simple composition and achieved optimal separation of DBM and the I.S. CHMPP without interference from other components in rat plasma (Figure 3.3). The final flow rate and gradient mobile Phase condition were chosen to achieve balanced

results in terms of peak shape, resolution and sensitivity of DBM as well as I.S. CHMPP (Table 3.1). Carry-over in the assay was evaluated by checking blank plasma sample after injection of QC samples at high concentration, no significant carry-over (less than 0.3%) was found.

Liquid-liquid extraction method was used for sample preparation, the extraction solution ethyl acetate/methanol (95:5 v/v) was chosen based on previous study in which the same solvent was used to extract the β-diketone analogue curcumin [55]. For the reconstitution buffer, initially a solution of starting mobile Phase (A:B, 95:5, v/v) was used, but the peak area of both DBM and CHMPP was much less than using the acetonitrile/water (50:50) as reconstitution buffer, therefore the latter was chosen for the assay. These selected conditions of sample preparation and liquid chromatographic conditions enabled the establishment of the LLOQ of DBM as low as 0.05 μg/mL by using 50 μL of rat plasma.

3.3.2 HPLC method validation

3.3.2.1 Specificity and selectivity

Figure 3.3 represents chromatograms of DBM and I.S. CHMPP from rat plasma after liquid-liquid extraction along with blank plasma sample. No interference of endogenous

peaks with DBM or CHMPP at their respective retention times (DBM t_R=21.417 min; CHMPP t_R=24.050 min) in blank rat plasma. The capacity factor (k) for analyte DBM and I.S. CHPMPP were 8.18 and 9.32, respectively. Figure 3.3C showed that there were no *in vivo* DBM metabolites interfering with the parent compound DBM and I.S.

3.3.2.2 Sensitivity

The lower limit of quantification (LLOQ) was defined as those quantities that were 10-fold above the background noise, with precision errors of less than 20% (CV) and inaccuracy between ± 20% (bias). The LLOQ of DBM extracted from 50 μL rat plasma was found to be 0.05 μg/mL after injection of 20 μL of the 100 μL reconstitutes. The mean percent accuracy value for plasma samples was 98% and precision coefficient of variation (CV) was below 10% at the LLOQ (Table 3.2).

3.3.2.3 Linearity of calibration curve

The calibration curves for DBM were linear over the concentration range of 0.05-20 μg/mL in rat plasma. The mean (± S.D.) regression equation from three replicate calibration curves on different days was y = (0.0015489 ± 0.000022)x + (0.0141 ± 0.0099) with correlation coefficient r^2 = 0.9995 ± 0.0006.

3.3.2.4 Precision and accuracy

Table 3.2 shows a summary of intra- and inter-day precision and accuracy. In the range of 0.05-20 μg/mL, intra- and inter-day accuracy ranged from 100.5-105.6 and 99.2-102.9%, respectively. Therefore, the intra- and inter-day accuracies (% deviation) were within ± 20% for the LLOQ and ± 15% for other QC samples. The intra- and inter-day assay precision (CV) ranged from 0.5-5.6 and 5.3-10.7% respectively, which were also within the acceptable range of 20% at LLOQ and 15% at other QC samples. The relative higher %CV in the inter-day analysis compared to the intra-day analysis (Table 3.2) is probably due to slight different composition of the reconstitute buffer acetonitrile/water (50:50, v/v) used at different days. These results indicated that the present assay has very good accuracy and precision.

3.3.2.4 Recovery

Absolute recovery was evaluated by comparison of the DBM/CHMPP peak area ratios of the extracted samples at the three QC levels with the standard solutions of equivalent concentrations. The mean extraction recovery of DBM was 80.6, 83.4 and 77.1% for low, medium and high QC samples, respectively.

3.3.2.5 Stability

DBM primary stock solution (1 mg/mL in methanol) was stable for at least 3 months (data not shown) at - 80°C. The stability study results of DBM under various conditions were summarized in Table 3.3. DBM at all QC levels was stable in rat plasma for 4 h at ambient temperature, after three freeze/thaw cycles, as well as after long-term storage at - 80°C for one month. DBM was also stable in the reconstituted buffer for 48 h in the autosampler at 4°C. The high stable property of DBM in rat plasma suggested no special care was needed during sample preparation. The high stability of DBM in reconstituted buffer at 4°C also suggested a large batch of samples could be processed at one time within 48 h, which would compensate for the shortcoming of relative long running time of this assay.

3.3.3 Application of the developed HPLC method for pharmacokinetics study

3.3.3.1 Pharmacokinetics Studies of DBM after Intravenous Administration

With LLOQ of 0.05 μg/mL, plasma concentrations of DBM in pharmacokinetics study were successfully quantified by the assay up to 24 h (concentrations in 36 h samples were below LLOQ). The mean concentration-time profiles of DBM after intravenous administration of 10 and 20 mg/kg in rats are shown on Figure 3.4. The

pharmacokinetic parameters determined by noncompartmental analysis are summarized in Table 3.4. Following intravenous administration at dose of 10 and 20 mg/kg, $AUC_{0\rightarrow\infty}$ values were 16.52 and 27.89 hr×μg/mL, respectively. The dose-normalized plasma concentration-time profiles, presented in Figure 3.5, were superimposable. In addition, dose-normalized AUC values were 1.65 and 1.40 at doses of 10 and 20 mg/kg, which is not significant between 10 and 20 mg/kg. These results suggest that DBM follows linear pharmacokinetics within the dose ranges tested.

Following intravenous administration of 10 and 20 mg/kg, DBM was eliminated with systemic clearance of 0.71 and 0.72 L/hr/kg and $t_{1/2}$ of 14.4 and 12.0 h. The clearance of DBM remained unchanged with increased dose. The half life values are also not significant different. The steady state volume of distribution of DBM was 6.75 and 7.35 L at doses of 10 and 20 mg/kg. The values are greater than total body water of 0.67 L/kg, suggesting that DBM may be widely distributed into tissue. These parameters suggested that DBM is a low clearance compound with high volume of distribution in SD rats. MRT value of 10 mg/kg is 10.4 hr, similar to that of 20 mg/kg (10.2 hr). Therefore, DBM shows very similar pharmacokinetic patterns between 10 and 20mg/kg.

3.3.3.2 Pharmacokinetics Studies of DBM after Oral Administration

The mean concentration-time profiles of DBM after oral administration of 10, 50, and 250 mg/kg in rats are shown on Figure 3.6. Noncompartmental analysis was performed to obtain basic pharmacokinetic parameters listed in Table 3.5. Following oral administration at 10, 50 and 250 mg/kg, DBM was absorbed and reached Cmax of 10.55, 12.71, and 13.69 μg/mL at Tmax of 2, 2, and 3.3 h, respectively. The $AUC_{0\rightarrow\infty}$ values were 2.25, 9.46, 31.89 hr×μg/mL at doses of 10, 50, and 250 mg/kg. The increase of Cmax and $AUC_{0\rightarrow\infty}$ were not proportional to the increase of dose. The MRT values at two lower doses are smaller than that of highest dose, suggesting that it takes more time to be absorbed at higher dose. The half life remained unchanged when the dose increased. Following oral administration of 10 mg/kg DBM, *ka* was calculated as 2.86 h^{-1}. Absolute bioavailability (F) of DBM was estimated to be 13.62, 11.45, and 7.72% at doses of 10, 50, and 250 mg/kg, respectively, indicating that the mechanism of low absorption in the intestine or extensive gut/liver metabolism may be involved. This lower extent of absorption could be related to its lower solubility in water as well.

3.4 Conclusion

A simple, sensitive, accurate and precise HPLC method was developed and

validated for the first time to quantify DBM in rat plasma. Simple liquid-liquid extraction method was used to prepare the samples and a Gemini C18 column was used to analyze the samples. The present method was applied successfully to a pharmacokinetic study of DBM in the rats, in which basic pharmacokinetic parameters such as absolute bioavailability, clearance, terminal half life, steady state volume of distribution etc. were determined. This pharmacokinetic study suggested that DBM is widely distributed into the tissue and that the process of absorption may involve the first-pass effect with the low absolute bioavailability. The chromatographic condition as well as sample preparation method of the current assay will likely facilitate the development and validation of HPLC-UV analytical assays to analyze DBM in other biological matrixes such as urine and tissue homogenates, which will be our future studies.

Table3.1 HPLC mobile Phase gradient conditions for analysis of DBM

Time (min)	Flow rate (mL/min)	% A	% B
0	0.2	95	5
15	0.2	0	100
20	0.2	0	100
21	0.2	95	5
30	0.2	95	5

Mobile Phase A: water/methanol (80:20, v/v) with 0.1% TFA

Mobile Phase B: acetonitrile with 0.1% TFA

Table 3.2 The intra- and inter-day accuracy and precision of QC samples (*n=3*)

	Added Concentration (μg/mL)	Measured Concentration (μg/mL)	Accuracy (%)	CV (%)
Intra-day	0.05	0.0528 ± 0.0054	105.6	5.6
	1	1.0085 ± 0.0326	100.9	0.9
	20	20.1070 ± 0.8835	100.5	0.5
Inter-day	0.05	0.0496 ± 0.0053	99.2	10.7
	1	1.0288 ± 0.0639	102.9	6.2
	20	20.5771 ± 1.0851	102.9	5.3

Table 3.3 Stability of DBM at various experimental conditions

QC sample	Stability condition	% Remaining ± SD
0.05 μg/ml	4 h at room temperature	98.9 ± 10.5
	3 freeze-thaw cycles	95.7 ± 11.5
	30 days storage at – 80 °C	98.5 ± 5.9
	48 h in autosampler at 4 °C	98.6 ± 7.5
1 μg/ml	4 h at room temperature	95.1 ± 4.5
	3 freeze-thaw cycles	99.4 ± 1.2
	30 days storage at – 80 °C	107.9 ± 3.0
	48 h in autosampler at 4 °C	100.5 ± 2.6
20 μg/ml	4 h at room temperature	96.3 ± 1.3
	3 freeze-thaw cycles	102.4 ± 1.2
	30 days storage at – 80 °C	109.8 ± 2.1
	48 h in autosampler at 4 °C	100.7 ± 3.5

Table 3.4 Pharmacokinetics parameters of DBM after intravenous administration determined by Noncompartmental Analysis. Statistics were conducted by ANOVA followed by Bonferroni's test, $n = 4$.

Dose (mg/Kg)	10 ($n = 4$)	20 ($n = 4$)
AUC (hr×μg/mL)	16.52 ± 7.85	27.98 ± 2.40
t1/2 (hr)	14.43 ± 5.00	12.02 ± 5.34
Cl (L/hr/Kg)	0.71 ± 0.32	0.72 ± 0.07
Vss (L/Kg)	6.75 ± 1.85	7.35 ± 4.26
MRT (hr)	10.43 ± 3.33	10.19 ± 6.10
AUC/Dose	1.65	1.40

Table 3.5 Pharmacokinetics parameters of DBM after oral administration determined by Noncompartmental Analysis. Statistics were conducted by ANOVA followed by Bonferroni's test, $n = 3$ or 4.

Dose (mg/Kg)	10 ($n = 4$)	50 ($n = 3$)	250 ($n = 3$)
AUC (hr×μg/mL)	2.25 ± 0.33	9.46 ± 1.62	31.89 ± 6.89
t1/2 (hr)	10.55 ± 3.37	12.70 ± 4.15	13.68 ± 3.77
Tmax (hr)	2.00 ± 1.35	2.00 ± 0.00	3.33 ± 1.15
Cmax (μg/mL)	0.34 ± 0.04	1.50 ± 0.41	2.88 ± 0.74
MRT (hr)	10.78 ± 3.03	9.37 ± 1.98	18.02 ± 1.62*,**
F (%)	13.62	11.45	7.72

*$p<0.05$ compared to the group administered with 10 mg/Kg DBM.

**$P<0.05$ compared to the group administered with 50 mg/Kg DBM.

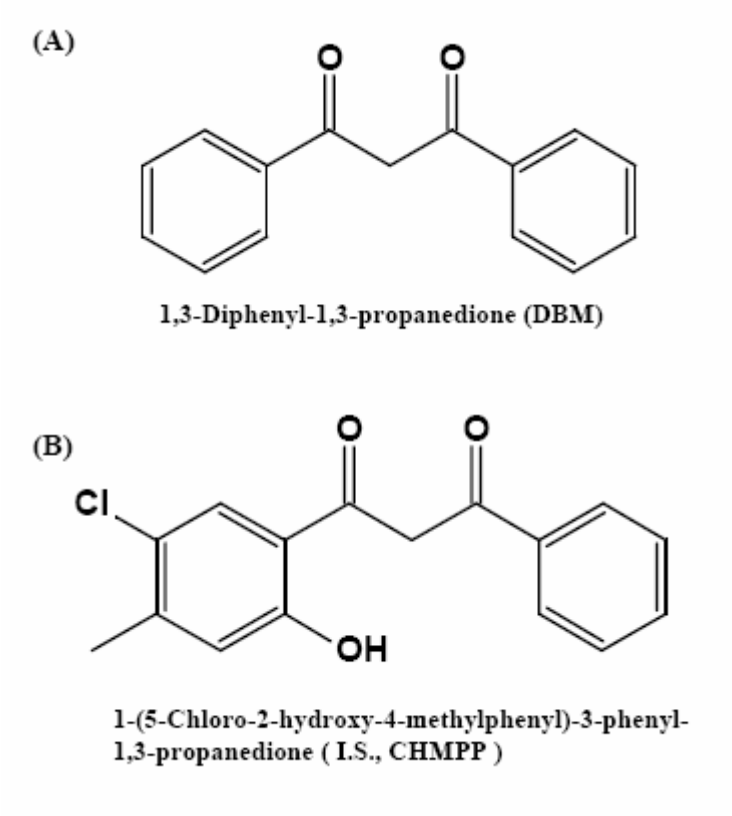

Figure 3.1 chemical structures of DBM (A) and internal standard CHMPP (B).

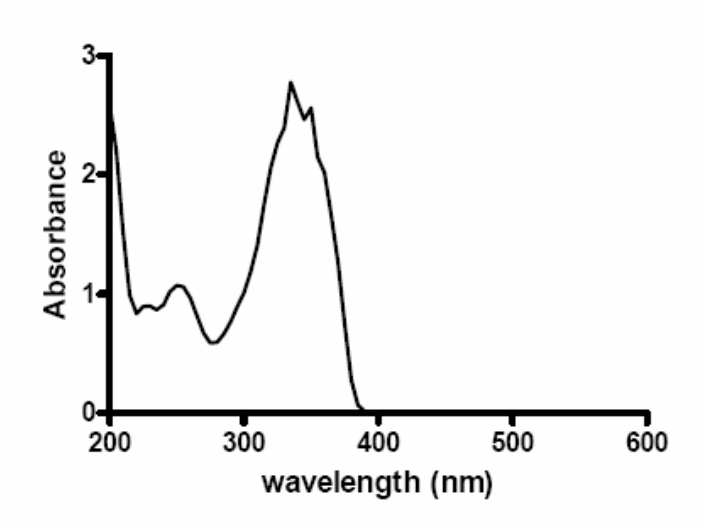

Figure 3.2 UV-Vis absorption spectra (200-500nm) of DBM in acetonitrile (25 μg/mL).

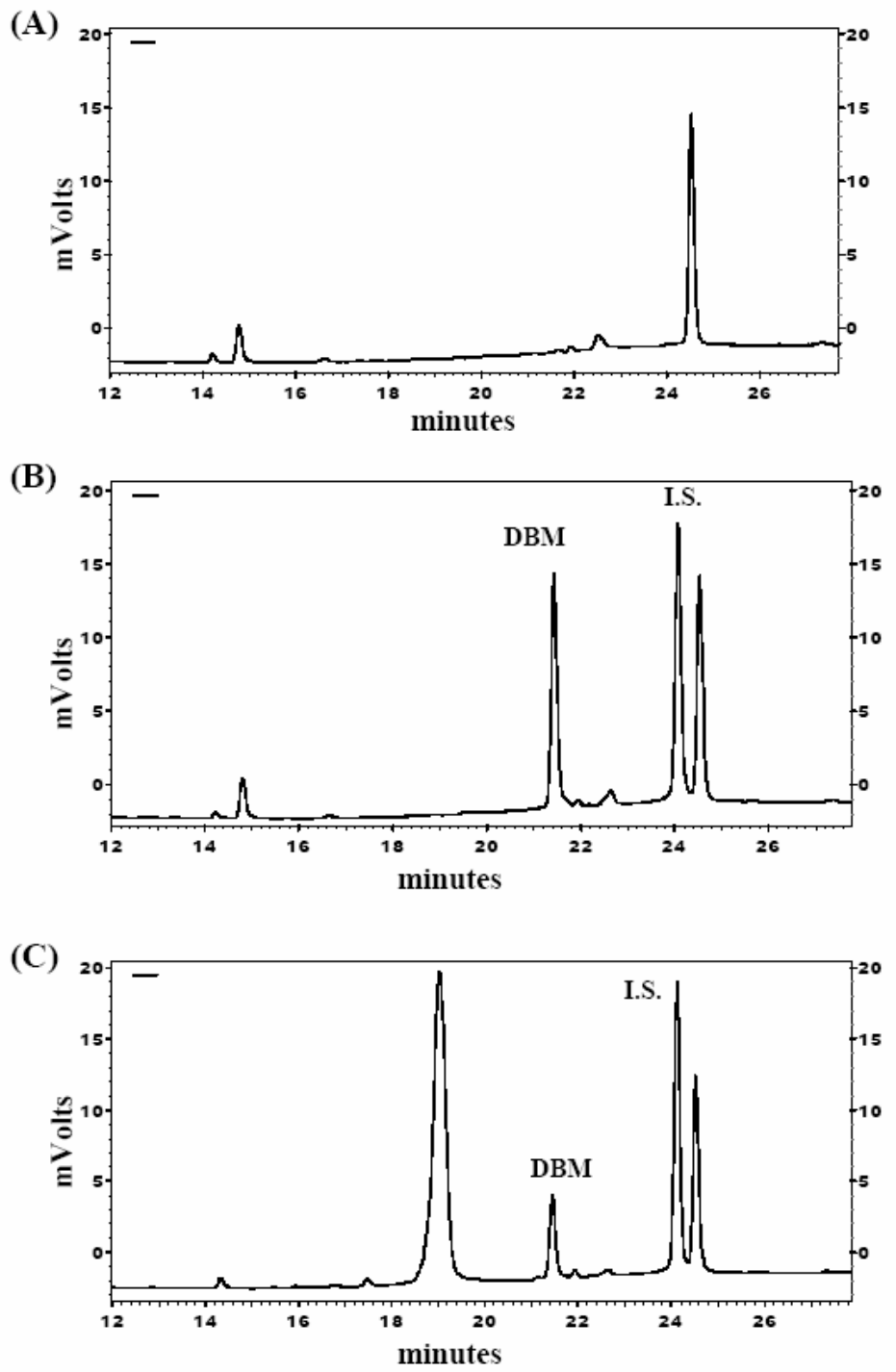

Figure 3.3 Representative chromatograms of: (A) blank rat plasma; (B) blank rat plasma spiked with DBM (0.5 μg/mL) and internal standard (I.S.) CHMPP (2 μg/mL); and (C) rat plasma sample at 8 h after oral administration of DBM at dose of 50 mg/kg and spiked with 2 μg/mL I.S. CHMPP.

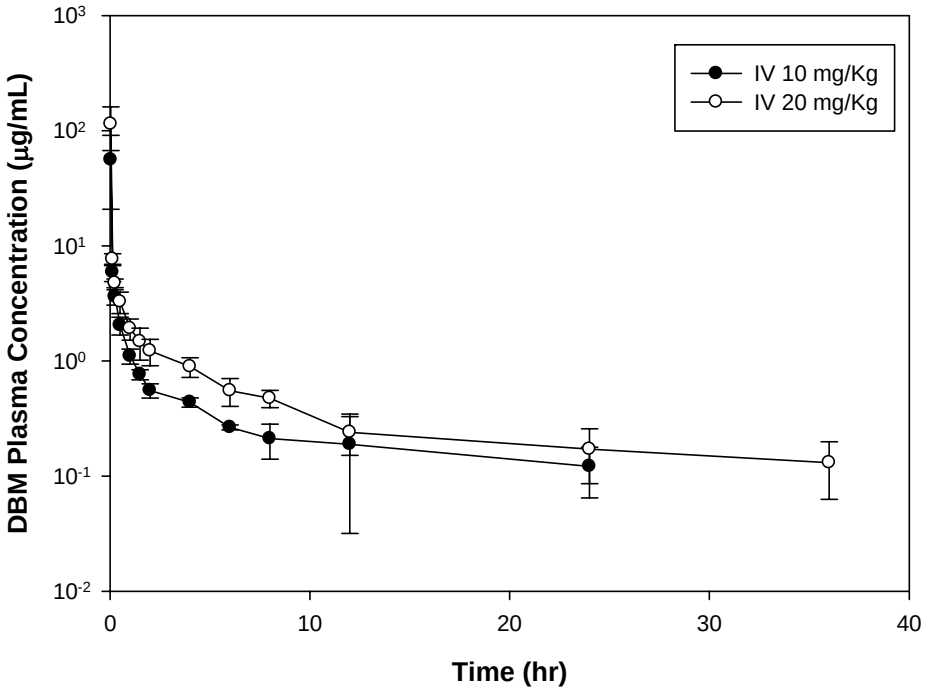

Figure 3.4 The plasma concentration profile of DBM after intravenous administration. Rats were dosed intravenously with 10 or 20 mg/Kg of DBM. Data were expressed as mean ± SD, n = 4.

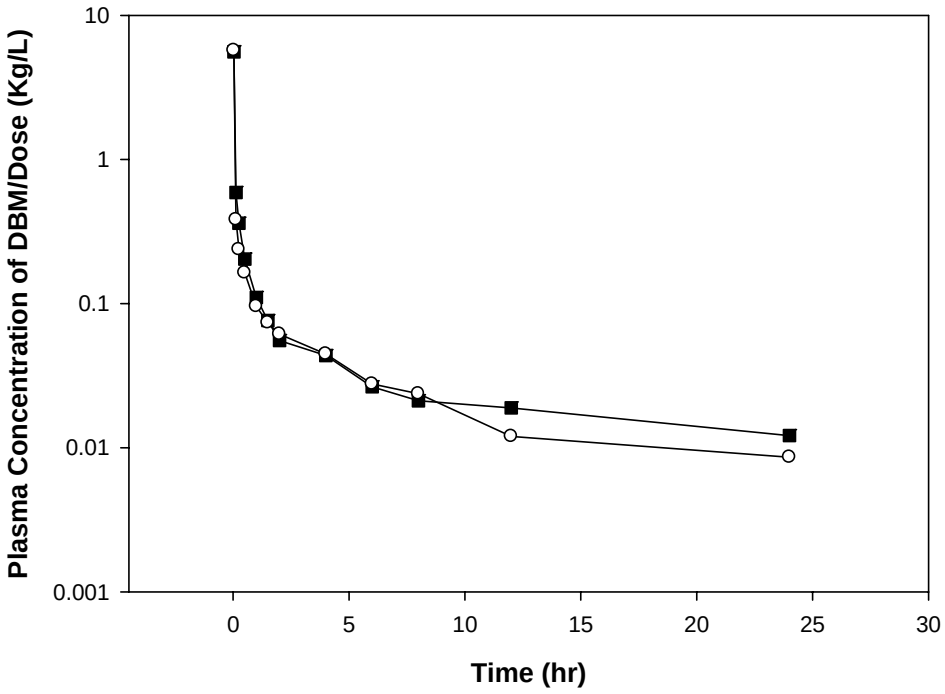

Figure 3.5 The dose-normalized plasma concentration of DBM in rats after intravenous administration. Rats were dosed with 10 (■) and 20 (○) mg/Kg of DBM.

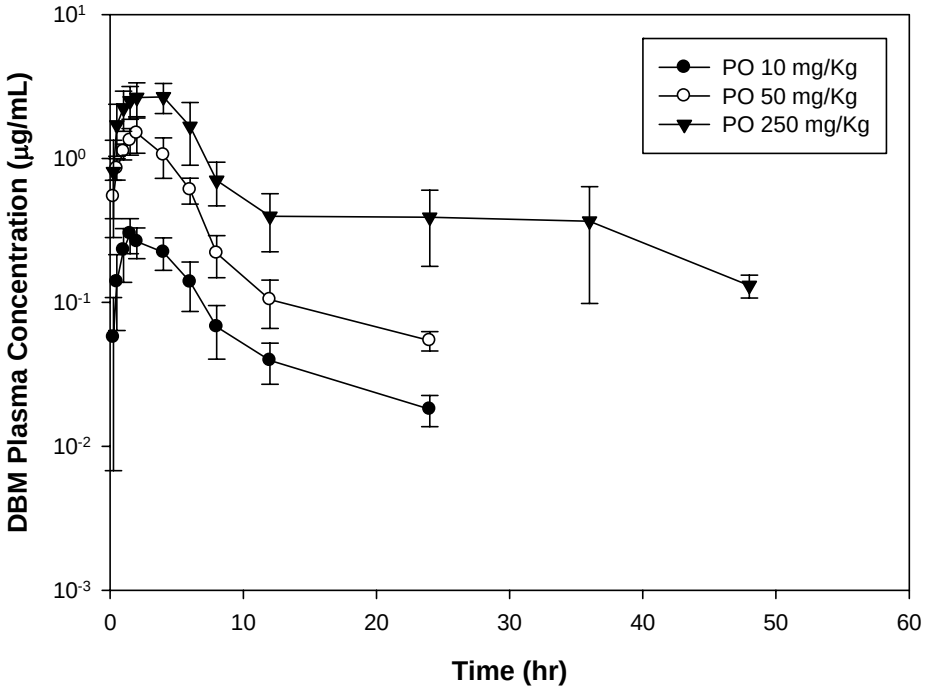

Figure 3.6 The plasma concentration profile of DBM after oral administration. Rats were dosed by oral gavage with 10, 50, or 250 mg/Kg of DBM. Data are expressed as mean ± SD, n = 3 or 4.

APPENDIX

A.1 Two Compartmental Model Analyses

Compartmental analysis was also conducted using WinNonlin v.4.0. The appropriate model was determined following the goodness of fit including visual inspection, Akaike's Information Criterion (AIC), and correlation coefficient (r^2). The plasma versus time profiles were fitted to a two compartmental model with elimination from the central compartment. Nonlinear regression analysis was performed using the simplex algorithm of Nelder and Mead method and the weighting factor of $1/C^2$ in model fitting. Initial parameters were estimated from noncompartmental analysis. Primary parameters derived form the two compartmental model included the first order absorption rate constant (K_{01}), volume of distribution in the central compartment (V_c), peripheral distribution constant (K_{12}, K_{21}), and elimination rate constant (K_{10}).

A.2 Two Compartmental Modeling of DBM Plasma Concentration-Time Profiles

One compartmental and two compartmental model with elimination from the central compartment were used to simultaneously fit the plasma concentration versus time

profiles following intravenous and oral administration as shown in Figure A.1 (page 68). The two compartment model provided better fit based on goodness of fit including the lower AIC criteria and the better correlation coefficient. The primary estimated pharmacokinetic parameters obtained following two compartment analysis are summarized in Table A.1 (page 67). The observed and predicted plasma concentrations of DBM after intravenous and oral administration are shown in Figure A.2.

Following the intravenous administration of DBM at doses of 10 and 20 mg/kg, the volume of distribution of the central compartment (V_c) of DBM was 0.44 and 0.08 L/Kg, respectively. These values were much smaller than the volume of distribution at steady state (0.76 L/kg). The peripheral compartment (V_p) (0.49, 0.61 L/Kg) was also higher than V_c. The k_{12}/k_{21} ratio has a high value of 26.3 and 46.2 for 10 and 20 mg/Kg, respectively. These results suggested that DBM may widely distribute to the peripheral tissues.

The plasma versus time profiles following oral administration were also fitted to a two compartmental model. The first order absorption rat constant (K_{01}) was 0.68, 0.55, and 0.54 h^{-1} at the doses of 10, 50, and 250 mg/kg, respectively. The volume of distribution of the central compartment obtained following the oral administration was similar to that following the intravenous administration. Although the peripheral

distribution constants are much smaller than that following the intravenous administration, the k_{12}/k_{21} ratio is still a high value of 8, 19, 16 for 10, 50 and 250 mg/Kg, respectively. The first order elimination constant has a very small value (0.12, 0.23, 0.06 h^{-1} for 10, 50, 250 mg/kg, respectively) and V_p was still larger that V_c. These results suggest that DBM is retained in the peripheral tissues following the oral as well as the intravenous administrations.

Table A.1 Estimated pharmacokinetics parameters of DBM in rats after intravenous and oral administration determined by two compartmental analysis.

Parameters	IV group		PO group		
	10mg/Kg	20mg/Kg	10mg/Kg	50mg/Kg	250mg/Kg
Vc (L/Kg)	0.44	0.08	3.04	1.15	2.32
K01 (hr^{-1})	-	-	0.68	0.55	0.54
K10 (hr^{-1})	8.45	13.89	0.12	0.23	0.06
K12 (hr^{-1})	9.73	16.63	0.24	0.38	0.32
K21 (hr^{-1})	0.37	0.36	0.03	0.02	0.02
Vp (L/Kg)	0.49	0.61	31.43	34.50	37.90

(A)

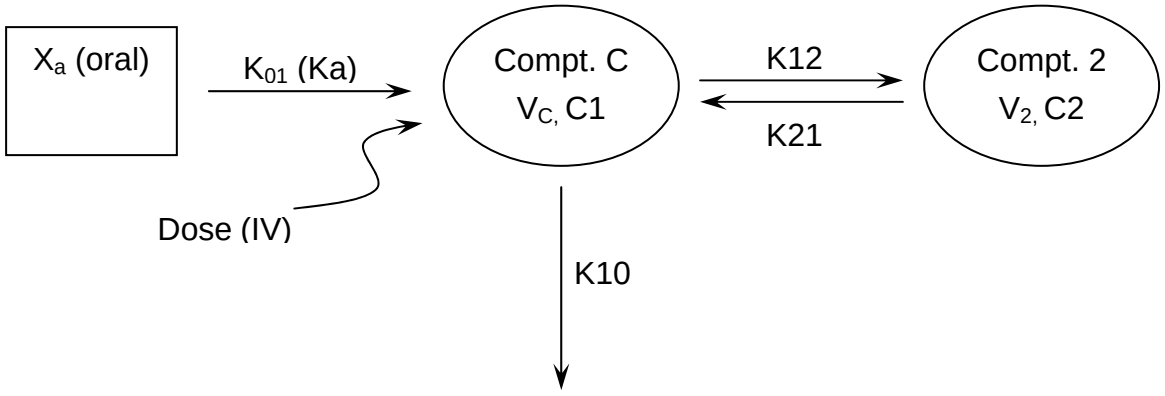

(B)

$$\frac{dXa}{dt} = -k01 \times Xa \qquad (Xa_{,0} = Xa) \qquad (1)$$

$$\frac{dC1}{dt} = k01 \times \frac{Xa}{Vc} + k21 \times C2 - (k12 + k10) \times C \quad (C_{1,0} = 0) \qquad (2)$$

$$\frac{dC1}{dt} = k21 \times C2 - (k12 + k10) \times C1 \quad (C_{1,0} = Xa/Vc) \qquad (3)$$

$$\frac{dC2}{dt} = k12 \times C1 - k21 \times C2 \quad (C_{2,0} = 0) \qquad (4)$$

Figure A.1 The two compartmental model (A) and the differential equations used for two compartmental mode. Xa represent the drug amount at the absorption site; C1 and C2 represent the plasma concentrations of DBM in central and peripheral compartments; k01 is the absorption rate constant; k12 and k21 is the distribution constant between central and peripheral compartments; k10 is the elimination constant. These initial conditions for each equation are shown in parenthesis. Equation (1), (2), and (4) were used to fit the oral data and equations (3), and (4) were used to fit the intravenous data.

(A)

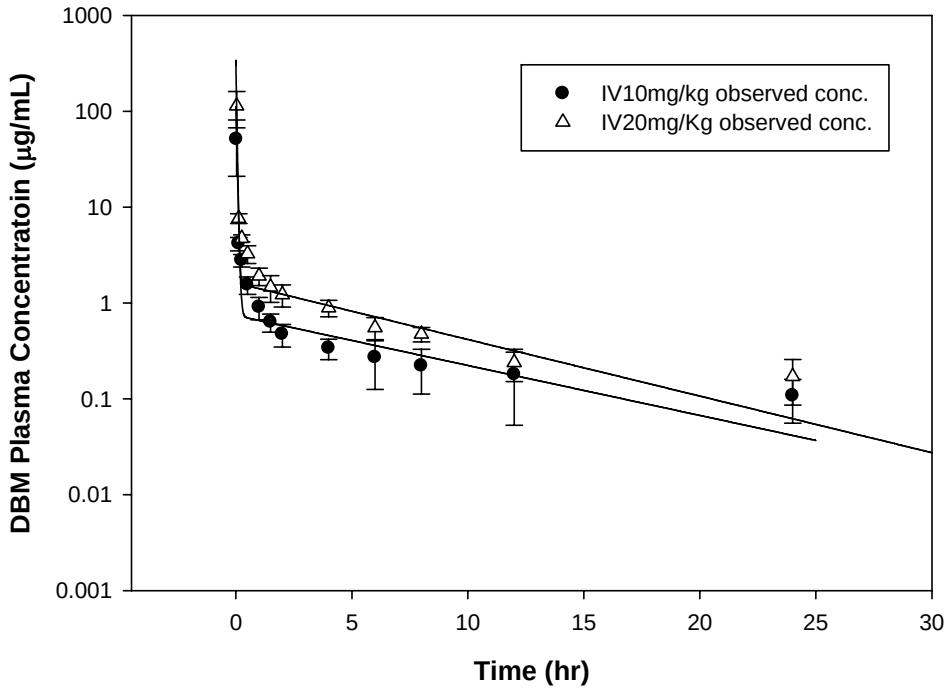

(B)

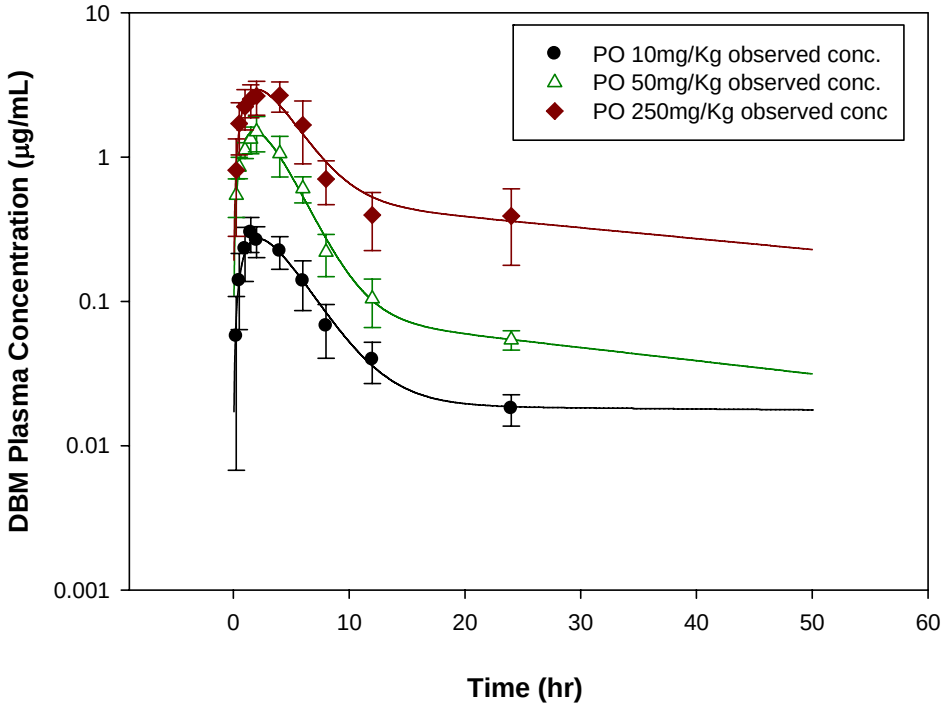

Figure A.2 Two compartmental Model fitting to the DBM Plasma concentration profile following intravenous (A) and oral administration (B). The lines represent predicted plasma DBM concentrations using the two compartmental model.

Reference

[1] Surh, Y.J. (2003) Nat Rev Cancer 3, 768-80.

[2] Klaassen, C.D., Watkins III, John B. (2003), pp. 116 McGraw Hill.

[3] Seymour, J.D., Calle, E.E., Flagg, E.W., Coates, R.J., Ford, E.S. and Thun, M.J. (2003) Am J Epidemiol 157, 980-8.

[4] Mandlekar, S., Hong, J.L. and Kong, A.N. (2006) Curr Drug Metab 7, 661-75.

[5] Greenwald, P. (2001) Toxicology 166, 37-45.

[6] Parkin, D.M., Bray, F., Ferlay, J. and Pisani, P. (2005) CA Cancer J Clin 55, 74-108.

[7] (2006) American Cancer Society, Altanta, Georgia.

[8] Giovannucci, E. (2002) Gastroenterol Clin North Am 31, 925-43.

[9] Papapolychroniadis, C. (2004) Tech Coloproctol 8 Suppl 1, s7-9.

[10] Shimizu, H., Mack, T.M., Ross, R.K. and Henderson, B.E. (1987) J Natl Cancer Inst 78, 223-8.

[11] Fearnhead, N.S., Wilding, J.L. and Bodmer, W.F. (2002) Br Med Bull 64, 27-43.

[12] Fearon, E.R. and Vogelstein, B. (1990) Cell 61, 759-67.

[13] Vogelstein, B. and Kinzler, K.W. (1993) Trends Genet 9, 138-41.

[14] T. Fukai, J.N., T. Nomura (1994) Phytochemistry 35, 515-519.

[15] Dinkova-Kostova, A.T. and Talalay, P. (1999) Carcinogenesis 20, 911-4.

[16] Lin, C.C., Ho, C.T. and Huang, M.T. (2001) Proc Natl Sci Counc Repub China B 25, 158-65.

[17] Huang, M.T. et al. (1998) Carcinogenesis 19, 1697-700.

[18] Shen, G. (2006) in: Pharmaceutical Sciences, Vol. doctor of philosophy, pp. 145-179 Rutgers, the state university of New Jersey, Piscataway.

[19] Lin, C.C., Tsai, Y.L., Huang, M.T., Lu, Y.P., Ho, C.T., Tseng, S.F. and Teng, S.C. (2006) Carcinogenesis 27, 131-6.

[20] Lin, C.C., Lu, Y.P., Lou, Y.R., Ho, C.T., Newmark, H.H., MacDonald, C., Singletary, K.W. and Huang, M.T. (2001) Cancer Lett 168, 125-32.

[21] Singletary, K., MacDonald, C., Iovinelli, M., Fisher, C. and Wallig, M. (1998) Carcinogenesis 19, 1039-43.

[22] Lenoir, V., de Jonage-Canonico, M.B., Perrin, M.H., Martin, A., Scholler, R. and Kerdelhue, B. (2005) Breast Cancer Res 7, R470-6.

[23] Toniolo, P.G., Levitz, M., Zeleniuch-Jacquotte, A., Banerjee, S., Koenig, K.L., Shore, R.E., Strax, P. and Pasternack, B.S. (1995) J Natl Cancer Inst 87, 190-7.

[24] Dorgan, J.F. et al. (1996) Cancer Epidemiol Biomarkers Prev 5, 533-9.

[25] Perillo, B., Sasso, A., Abbondanza, C. and Palumbo, G. (2000) Mol Cell Biol 20, 2890-901.
[26] Pethe, V. and Shekhar, P.V. (1999) J Biol Chem 274, 30969-78.
[27] King, R.S., Teitel, C.H., Shaddock, J.G., Casciano, D.A. and Kadlubar, F.F. (1999) Cancer Lett 143, 167-71.
[28] MacDonald, C.J., Ciolino, H.P. and Yeh, G.C. (2001) Cancer Res 61, 3919-24.
[29] Sogawa, K. and Fujii-Kuriyama, Y. (1997) J Biochem (Tokyo) 122, 1075-9.
[30] Jackson, K.M., DeLeon, M., Verret, C.R. and Harris, W.B. (2002) Cancer Lett 178, 161-5.
[31] Frazier, M.C., Jackson, K.M., Jankowska-Stephens, E., Anderson, M.G. and Harris, W.B. (2004) Proteomics 4, 2814-21.
[32] Harvey Lodish, M.P.S., Paul Matsudaira, James Darnell, Lawrence Zipursky, Chris A. Kaiser, Arnold Berk, Monty Krieger (2003) W. H. Freeman.
[33] Pardee, A.B. (1989) Science 246, 603-8.
[34] Johnson, D.G. and Walker, C.L. (1999) Annu Rev Pharmacol Toxicol 39, 295-312.
[35] Malumbres, M. and Barbacid, M. (2001) Nat Rev Cancer 1, 222-31.
[36] Kato, J., Matsushime, H., Hiebert, S.W., Ewen, M.E. and Sherr, C.J. (1993) Genes Dev 7, 331-42.
[37] Weinberg, R.A. (1995) Cell 81, 323-30.
[38] Mittnacht, S., Lees, J.A., Desai, D., Harlow, E., Morgan, D.O. and Weinberg, R.A. (1994) Embo J 13, 118-27.
[39] Kohn, K.W. (1999) Mol Biol Cell 10, 2703-34.
[40] Yam, C.H., Fung, T.K. and Poon, R.Y. (2002) Cell Mol Life Sci 59, 1317-26.
[41] Fung, T.K. and Poon, R.Y. (2005) Semin Cell Dev Biol 16, 335-42.
[42] Pommier, Y. and Kohn, K.W. (2003) Med Sci (Paris) 19, 173-86.
[43] Sherr, C.J. and Roberts, J.M. (1999) Genes Dev 13, 1501-12.
[44] Kaldis, P. (1999) Cell Mol Life Sci 55, 284-96.
[45] Nasi, S., Ciarapica, R., Jucker, R., Rosati, J. and Soucek, L. (2001) FEBS Lett 490, 153-62.
[46] Sears, R.C. (2004) Cell Cycle 3, 1133-7.
[47] Reed, S.I. (2006) Results Probl Cell Differ 42, 147-81.
[48] Shen, G., Khor, T.O., Hu, R., Yu, S., Nair, S., Ho, C.T., Reddy, B.S., Huang, M.T., Newmark, H.L. and Kong, A.N.T. (2007 (summitted)).
[49] Pan, M.H., Huang, M.C., Wang, Y.J., Lin, J.K. and Lin, C.H. (2003) J Agric Food Chem 51, 3977-84.
[50] Geng, Y., Yu, Q., Sicinska, E., Das, M., Bronson, R.T. and Sicinski, P. (2001) Proc

Natl Acad Sci U S A 98, 194-9.

[51] Wong, H., Anderson, W.D., Cheng, T. and Riabowol, K.T. (1994) Anal Biochem 223, 251-8.

[52] Moretti, R.M., Marelli, M.M., Motta, M., Polizzi, D., Monestiroli, S., Pratesi, G. and Limonta, P. (2001) Prostate 46, 327-35.

[53] Rodriguez-Antona, C., Donato, M.T., Pareja, E., Gomez-Lechon, M.J. and Castell, J.V. (2001) Arch Biochem Biophys 393, 308-15.

[54] Chen, C. and Kong, A.N. (2005) Trends Pharmacol Sci 26, 318-26.

[55] Heath, D.D., Pruitt, M.A., Brenner, D.E. and Rock, C.L. (2003) J Chromatogr B Analyt Technol Biomed Life Sci 783, 287-95.

Curriculum Vita

JIN-LIERN HONG

EDUCATION

2000-2004 B.S., Pharmacy, Kaohsiung Medical University, Taiwan
2004-2007 M.S., Pharmaceutical Sciences, Rutgers, The State University of New Jersey

PUBLICATIONS

- Mandlekar, S, **Hong, JL.** and Kong, AN. Modulation of metabolic enzymes by dietary phytochemicals: a review of mechanisms underlying beneficial versus unfavorable effects. Curr Drug Metab. 7(6):661-75, 2006.
- Shen, G., **Hong, JL.** and Kong, A.N. High-performance liquid chromatographic method for the determination and pharmacokinetics study of dibenzoylmenthane (DBM). J. Chromatography B. 2007 Jan 10.